



Quantitative Proteomic Profiling of Stress and Immunological Responses in Target Organs Reveals How Myxozoan Parasites Determine the Outcome of Rainbow Trout Co-Infections

Mona Saleh^{*1}, Karin Hummel², Sarah Schlosser², Ebrahim Razzazi-Fazeli², Jerri L Bartholomew³, Christopher J. Secombes⁴, Mansour El-Matbouli¹

Abstract

In this study, we explore how myxozoan parasites modulate the host proteome landscape and immune responses at the target organs, thereby determining the outcome of co-infections in rainbow trout. Kidney and head cartilage samples were collected from five fish groups. In group 1, fish were infected with *M. cerebralis* (Mc), while fish in group 2 were exposed to *T. bryosalmonae* spores (Tb). Thirty days after infection, half of the fish from group 1 and group 2 were reciprocally co-infected with the other parasite, establishing group 3 (Mc+) and group 4 (Tb+). Group 5 fish were mock exposed to specific pathogen-free water and used as a negative control (C). In the head cartilage, upregulated proteins are involved in signal transduction, immune response, and host protection against oxidative stress, while the downregulated molecules are associated with cytoskeleton organization, DNA and RNA repair, protein folding, and metabolism. In the kidney, upregulated proteins are mainly involved in signal transduction, host immunity, DNA and RNA repair, and protection against oxidative stress. The downregulated proteins are mainly associated with extracellular matrix (ECM), cytoskeleton organization, and metabolism. This study provides the first proteomic profiles of rainbow trout responses to single and co-infections with *M. cerebralis* and *T. bryosalmonae* at the target organs. It delivers key information on how these two parasites trigger distinct immune signaling pathways and enhances our understanding of the host myxozoan interactions in single and co-infections, potentially enabling the development of effective interventions and therapeutic strategies for WD and PKD management in salmonid aquaculture.

Keywords: Salmonids, host-parasite interactions, proliferative kidney disease, proteome, whirling disease

Introduction

Whirling disease (WD) significantly impacts wild and cultured salmonid fish. It is induced by the myxozoan parasite *Myxobolus cerebralis*, a member of the class Myxosporidia [1, 2], which needs two hosts to complete its life cycle: a vertebrate salmonid and the invertebrate oligochaete *Tubifex tubifex* [3]. The head cartilage is the target organ for *M. cerebralis* in the fish host. Climate change suits the lifecycle conditions of this myxozoan parasite, resulting in significant effects on salmonid aquaculture and the decline of wild trout populations in North America and Europe [4, 5, 6, 7, 8]. Previous gene expression studies have examined the host immunological responses after

Affiliation:

¹Division of Fish Health, University of Veterinary Medicine, 1210 Vienna, Austria

²VetCore / Mass Spectrometry, University of Veterinary Medicine, 1210 Vienna, Austria

³Department of Microbiology, Oregon State University, Corvallis, OR, United States of America

⁴Scottish Fish Immunology Research Centre, School of Biological Sciences, University of Aberdeen, Scotland, UK

*Corresponding author:

Mona Saleh, Division of Fish Health, Department for Farm Animals and Veterinary Public Health, University of Veterinary Medicine, Austria.

Citation: Mona Saleh, Karin Hummel, Sarah Schlosser, Ebrahim Razzazi-Fazeli, Jerri L Bartholomew, Christopher J. Secombes, Mansour El-Matbouli. Quantitative Proteomic Profiling of Stress and Immunological Responses in Target Organs Reveals How Myxozoan Parasites Determine the Outcome of Rainbow Trout Co-Infections. Archives of Microbiology and Immunology. 9 (2026): 56-79.

Received: March 26, 2026

Accepted: April 01, 2026

Published: April 28, 2026

exposure to *M. cerebralis* [9, 10, 11, 12, 13, 14, 15]. Strong local and systemic immune responses, along with activation of T lymphocytes, especially CD4+ T helper cells, are crucial for host defense during WD. *M. cerebralis* elicits early cellular responses at infection sites, leading to pronounced local inflammatory reactions that likely exacerbate tissue damage inflicted by the parasite and facilitate its immune evasion and proliferation [16]. The control of Th17 immunity via the STAT3/SOCS-3/IL-6 pathway and the activation of SOCS-3 is a significant evasion technique employed by *M. cerebralis*, influencing the equilibrium between Treg cells and pro-inflammatory Th17 cells [14]. A balance between Th17 and Treg responses is essential for establishing protective immunity and enhancing WD resistance.

Proliferative kidney disease (PKD) is induced by the myxozoan *Tetracapsuloides bryosalmonae*, a member of the class Malacosporea [17]. *T. bryosalmonae* alternates between an invertebrate host, the freshwater bryozoan *Fredericella sultana*, and a vertebrate salmonid host [18, 19]. The kidney is the target organ for *T. bryosalmonae* in the fish host. PKD is defined by chronic immunopathology, granulomatous-like lesions, and lymphocytic hyperplasia [20]. Fish mortality may attain 95–100% during severe disease outbreaks, particularly when compounded by secondary illnesses and detrimental agricultural or environmental conditions [21, 22, 23], which can lead to economical and ecological impacts on fisheries and aquatic ecosystems. *T. bryosalmonae* are disseminated by robust hosts, including brown trout (*Salmo trutta*) in Europe, and through the transmission of infected bryozoans via statoblast dispersion and the mobility of infected zooids [24, 22, 25]. The pathophysiology of PKD is influenced by temperature; hence, its proliferation is exacerbated by climate change and rising temperatures [26, 27]. In particular, temperature promotes the development of *T. bryosalmonae* and other myxozoans, including *M. cerebralis*, in fish [28,8]. *T. bryosalmonae* modulates the transcription of essential genes related to T-helper (Th)-like functions, and Treg-like and Th17-like cytokines could play key roles in PKD pathogenesis in rainbow trout [26, 23]. In addition, during PKD, the JAK/STAT/SOCS axis is activated, and the transcripts of SOCS-1 and SOCS-3 are significantly upregulated, correlating with parasitic load and disease development in the *T. bryosalmonae*-infected fish [26, 29].

Myxozoan parasites employ various strategies to evade fish immune systems, as reported by several research studies [30, 31]. However, further investigation is needed to fully elucidate the immune response of fish during both single and co-infections with myxozoans, the latter being well documented [7, 8, 29, 32, 33]. Infections with mixed myxozoan species, including *T. bryosalmonae*, *Sphaerospora truttae*, *Chloromyxum schurovi*, *Chloromyxum truttae*, and *Myxobolus* species, were previously reported [32].

Natural co-infections with myxospores of a *Myxobolus* sp. and *Henneguya* sp. of the pond-reared fish *Piaractus mesopotamicus* were also reported [33]. Further, multiple myxozoan parasites, particularly *Myxobolus* species, have been reported in neotropical fish in Mexico [34]. In the case of co-infection with *T. bryosalmonae* and *M. cerebralis*, as used in this study, the relationship may be either synergistic or antagonistic [29, 35, 8, 7]. Previous research has explored the effects of co-infection with these two myxozoans on the pathophysiology of rainbow trout [35]. In case of co-infection, the immune response triggered by one pathogen can influence the pathogenesis of subsequent infections, either inhibiting or enhancing the fish's immune response. The modulation of the immune response in rainbow trout at the transcript level has been examined during co-infection in the posterior kidney and cranial cartilages, the target tissues affected by PKD or WD pathogenesis [29]. While there is a general understanding of the cellular and cytokine responses of rainbow trout to these two myxozoans from such studies, the proteomic changes that underlie the immune responses of fish to myxozoan parasites remain largely uninvestigated. Recently, we have investigated the proteome of caudal fin and gill tissues following exposure to *M. cerebralis* and *T. bryosalmonae* during both single and co-infections, revealing previously unknown protein modifications within the fish host at these sites of parasite entry into the host. Indeed, these two myxozoans modulated host defense mechanisms at the portals of entry, resulting in the synthesis of unique host proteins during each co-infection [7, 8].

In the current study, we present the proteome profiling of infected rainbow trout in the target organs for *M. cerebralis* and *T. bryosalmonae*, the head cartilage [2] and kidney [17, 29]. This study provides important information on proteome modulation, biological processes, and distinct pathways activated by the infection. Exploring the respective differences between the infection groups helps us to understand important molecular traits specific to single and co-infections and gives insights into how the sequence of the infection modulates host responses, thereby influencing disease outcome in fish. The identified proteins can be used for the development of novel approaches for disease management in aquaculture.

Methods

Ethics statement

All experiments were performed under protocols approved by the Animal Experimentation Ethics Committee of Vienna University of Veterinary Medicine (BMBWF–2021-0.240.416).

Experiment design

Pathogen-free rainbow trout (90 days old, mean length 4.02 ± 0.26 cm, mean weight 0.6 ± 0.15 g) were placed in tanks

($n = 3$) with water at 15°C and fed floating trout pellets (Aqua Garant, Austria) at a rate of 1% body weight (BW) per day, as detailed in Saleh et al. (2024). The North American strain (TL) of rainbow trout (Forellenzucht Trostadt GmbH & Co. KG, Reureith, Germany), recognized for its vulnerability to myxozoan parasites, was utilized in the exposure experiment [36, 8]. The fish were acclimatized under controlled laboratory conditions in a 1000 L capacity tank at 15°C for 14 days with sufficient aeration. The fish were monitored thrice daily for indications of illness (uncoordinated swimming and lethargy) to provide the prompt evacuation and euthanasia of affected specimens as necessary. Kidney (target organ of *T. bryosalmonae*) and head cartilage (target organ of *M. cerebralis*) samples were previously collected from five distinct fish groups [8].

Rainbow trout in group 1 were infected with *M. cerebralis* (Mc) triactinomyxons (TAMs) (2000 TAMs/fish), whereas fish in group 2 were exposed to free *T. bryosalmonae* spores (Tb) released from 22 mature parasite sacs at 16°C [8]. The TAMs were collected using a 20 µm mesh sieve from our laboratory infected *T. tubifex* that had been exposed previously to spores of *M. cerebralis* obtained from infected rainbow trout [37]. *T. bryosalmonae* spores were released from mature parasite spore sacs that were collected from infected *F. sultana* colonies [38]. *F. sultana* colonies were obtained from our established laboratory cultures, which originated at the very beginning from a single clonal population in Germany [38].

Prior to the *in vivo* experiments, to confirm that fish are free from infectious agents, fish ($n = 10$) were randomly selected

and inspected for parasites through microscopic analysis of gill and skin scrapings as described in Saleh et al. (2024). In addition, prior to and at sampling time points, kidney swabs were also taken to ensure the absence of bacterial infections via culture on blood agar plates, as previously outlined [39]. Homogenates of the brain, whole viscera, spleen, and kidney were also analyzed for viral presence utilizing BF-2 and EPC cell lines in accordance with established cell culture protocols [40].

No bacterial agents or viruses were detected before or during the experiment. Thirty days post exposure (dpe), fifty percent ($n = 18$ randomly selected fish ($n = 6$) from each triplicate tank) of the fish from group 1 ($n = 36$ in triplicate tanks) initially infected with Mc (distributed in triplicate tanks) and group 2 ($n = 36$ infected with Tb) were reciprocally co-infected with the alternate parasite, resulting in two additional groups, group 3 (Mc+) ($n = 18$ in triplicate tanks with 6 fish) and group 4 (Tb+) ($n = 18$ in triplicate tanks with 6 fish). Mock-exposed fish (pathogen-free water) (Group 5) ($n =$ in triplicate tanks with 6 fish) served as a negative control (C), according to Saleh et al. (2024) (Fig. 1A). Fish ($n = 9 / 3$ fish were collected from triplicate tanks) were sampled from each group at 1 day post co-infection (1 dpc)/1 month post exposure (mpe) to single infections to monitor the early host responses and at 2 months post co-infections (mpc) (3 mpe), which typically show highest parasite loads [29], to monitor the host response modulation in regard to parasite proliferation at the target organs. The fish were euthanized using an overdose (300 mg/L) of buffered tricaine methane sulfonate (MS-222) and sampled (Fig. 1B).

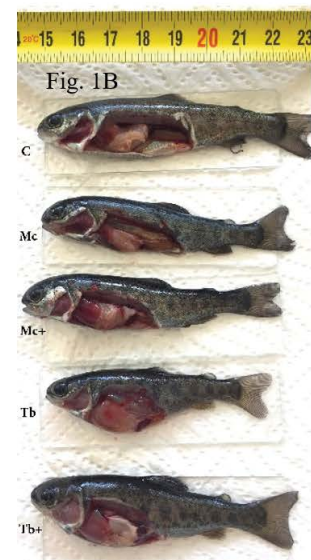
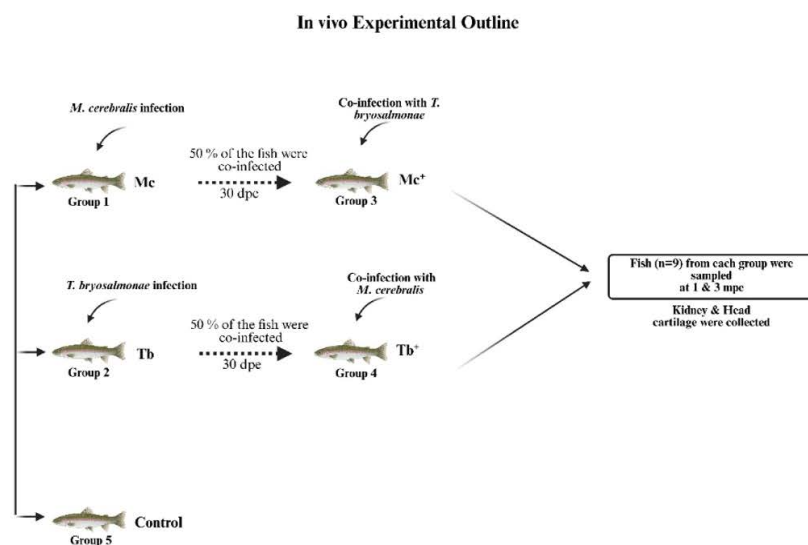


Figure 1: The outline of the *in vivo* experiment is presented (1A). The scheme shows the experimental design of the trial. The figure was created with BioRender.com. At 2 mpc (3 mpe), fish showed distinct clinical signs for each group, with single infection groups having typical clinical signs that were exacerbated in the co-infection groups (1B).

The head cartilage and kidney samples used in the current study were collected from the fish used in Saleh et al. (2024). In brief, the head cartilage and kidney samples were collected, rinsed with sterile phosphate buffer, and preserved in RNAlater (for RNA extraction) or frozen immediately in liquid nitrogen (for protein extraction) at -80°C .

cDNA synthesis and parasite load

Total RNA was isolated from head cartilage and kidney samples at each time point utilizing the RNeasy Mini Kit (Qiagen, Hilden, Germany) in accordance with the manufacturer's guidelines. An on-column DNase digestion step was conducted to eliminate any leftover DNA contamination. The RNA concentration and quality control were assessed using an agarose gel electrophoresis device (Thermo Fisher Scientific, Wilmington, USA) and a Nanodrop 2000c spectrophotometer. The iScript cDNA Synthesis Kit (Bio-Rad, Munich, Germany) was employed to synthesize cDNA from the isolated RNA in accordance with the manufacturer's instructions.

Prior to the exposure trial, ten fish were randomly selected, and the presence of *M. cerebralis* was assessed in the head cartilage, and *T. bryosalmonae* incidence was evaluated in the kidney, using qPCR as previously described [29]. The parasite load of *M. cerebralis* was assessed using cDNA samples derived from infected cranial cartilage. The forward primer Myx18-909 F (CTTTGACTGAATGTTATTACAGTTACAGCA) and the reverse primer Myx18-996 R (GCGGTCTGGGCAAATGC) were used. To determine the parasite load of *T. bryosalmonae* using cDNA samples derived from infected kidney, the forward primer RPL18 F (GTAAACGGGGACAAAAGA) and the reverse primer RPL18 R (GGAGCAGCACAAAATAC) were utilized, previously reported [26, 41]. RNA samples were efficiently used for assessing parasite load for the two myxozoans, acting as a marker for parasite viability and surpassing standard DNA-based methods [29, 8, 7]. For each PCR reaction, the total volume was 20 μL , which included 4 μL of 1:10 diluted cDNA, $1\times$ SsoAdvanced Universal SYBR Green Supermix (Bio-Rad), 0.4 μM of each primer, and DEPC-treated sterile distilled water (Bio-Rad). The PCR protocol consisted of an initial denaturation of cDNA at 95°C for 5 min, followed by 35 cycles of 95°C for 30 s, $57-62^{\circ}\text{C}$ for 30 s, and 72°C for 30 s. The detection thresholds for Myx18 and RPL18 were 35.89 and 37.50, respectively. A melting-point curve was generated, starting at 55°C and increasing by 0.5°C every 10 s until reaching 95°C , to assess non-specific binding using the CFX96 Touch Real-Time PCR detection system (Bio-Rad, Munich, Germany). Elongation factor 1 alpha was used as a reference gene for normalizing specific gene expression [35, 8, 7]. Relative gene expression was analyzed using CFX Manager software version 3.1 (Bio-Rad,

Munich, Germany). The relative gene expression changes of Myx18 and RPL18 were calculated using the comparative CT method ($2^{-\Delta\Delta\text{CT}}$) according to Livak and Schmittgen (2001). One-way analysis of variance (ANOVA) with Tukey's α -correction was used to examine the differences between the groups at each time point. The statistical differences were regarded as significant at a p -value ≤ 0.001 .

Protein extraction

Control and diseased fish tissue (50 mg) samples (head cartilage and kidney) were solubilized with 400 μL of pre-cooled denaturing lysis solution (7M urea, 2M thiourea, 4% CHAPS, and 1% DTT), augmented with a mammalian protease inhibitor cocktail (Sigma Aldrich, Vienna, Austria). Sample suspensions underwent disturbance via sonication. The lysates were preserved overnight at 4°C , vortexed, and centrifuged at $18,000\times g$ for 30 min at 4°C , with the supernatants collected. The total protein concentration of each lysate was determined colorimetrically with a DeNovix DS-11 FX+ spectrophotometer (DeNovix Inc., Wilmington, USA) and the Pierce 660 nm Protein Assay, adhering to the manufacturer's instructions (Thermo Scientific, Vienna, Austria).

Protein digestion and nanoLC-ESI-Orbitrap-MS/MS analysis

Digestion was executed utilizing the Filter-Aided-Sample Preparation (FASP) methodology as delineated by Ramires et al. (2022), in accordance with the methodologies established by Wiśniewski et al. (2009) and Wiśniewski (2016). A 10 kDa Pall Nanosep centrifugal device (Cytiva, MA, USA) was utilized to process 30 μg of protein. Promega's Trypsin-LysC-Mix (Wisconsin, USA) was utilized to digest proteins after reduction with dithiothreitol and alkylation with iodoacetamide. Peptides were extracted using three cycles of 50 μL 50 mM Tris, succeeded by centrifugation. Trifluoroacetic acid was utilized to acidify peptides to a pH under 2 before desalting and clean-up using Pierce C18 spin columns (Thermo Scientific, Vienna, Austria) according to the manufacturer's protocol. Peptides were separated using a nanoRSLC system equipped with a 25 cm Acclaim PepMap C18 column (Thermo Fisher) and subsequently detected using a high-resolution Q Exactive HF Orbitrap mass spectrometer (Thermo Fisher), as described in Gutiérrez et al. (2019).

Data Processing and quantification

The Proteome Discoverer Software version 2.4.1.15 from Thermo Fisher Scientific was employed to conduct the database search. The protein databases for *Oncorhynchus mykiss* (taxonomy ID 8022) and *Myxozoa* (taxonomy ID 35581) were taken from the UniProt website (<http://www.uniprot.org>). The search parameters were established as follows: The precursor mass tolerance was defined at 10 ppm,

and the fragment mass tolerance was set at 0.02 Da. Permitted dynamic changes encompassed the oxidation of methionine and N-terminal protein modifications, including acetylation, methionine loss, and their combinations. A static modification of carbamidomethylation on cysteine was employed. Protein identification was reported solely for proteins with at least two identified peptides.

The relative protein abundance in the experiments was evaluated using intensity-based label-free measurement. Protein abundance was determined from raw mass spectrometry data using Proteome Discoverer software and subsequently normalized to the total area summation. Before conducting additional statistical analysis using the R programming language per R Core Team (2021), we filtered the exported normalized abundance values in Excel to eliminate proteins with missing values. Modulated proteins showing pronounced elevated or reduced levels were involved in signal transduction, immune response, host protection against oxidative stress, extracellular matrix and cytoskeleton organization, protein folding, metabolism, or DNA repair; accordingly, the results were presented highlighting these functions.

Bioinformatic analysis of the differentially regulated proteins

Statistical evaluation was conducted in the R programming language to identify differentially expressed proteins in the trout tissue samples. One-way ANOVA was implemented to evaluate the differential expression of proteins for each protein. To mitigate the false discovery rate (FDR) and account for multiple testing, the Benjamini and Hochberg (1995) methodology was used. The differences were regarded significant if the FDR-adjusted p -values were less than the significance level of $\alpha = 0.001$. The honest significant difference method of Tukey was implemented as a post hoc test to evaluate the significance of the pairwise comparisons for these proteins. When the adjusted p -value of the ANOVA as well as of the Tukey post-hoc test of the respective comparison was less than α and the absolute fold change was at least two (fold change ≤ -2 or $\geq +2$), protein expression was regarded as modulated. The dataset has been submitted to the ProteomeXchange [42]. Consortium via the PRIDE [43] partner repository [44]. The dataset identifier (xxxx) has been assigned to the proteomics data obtained from mass spectrometry. The modulated proteins were allocated molecular functions, cellular components, and biological processes.

To identify pathways that were potentially modulated, the Kyoto Encyclopedia of Genes and Genomes (KEGG) PATHWAY database was implemented. The protein-protein functional interaction network of the differentially regulated proteins was determined using STRING v11.0

[45] to evaluate their amino acid sequences. The protein-protein network representation was examined by database analysis, experimental methods, text mining, co-expression, neighborhood analysis, gene fusion, and co-occurrence.

Results

Parasite burden

In head cartilage, the relative expression of *M. cerebralis* 18S rRNA was measured in single and coinfecting fish. The Mc+ groups exhibited the maximum loads of *M. cerebralis* at 1 dpc and 2 mpc (1 and 3 mpe), while the Mc group exhibited the lowest parasite count at 1 mpe. At 3 mpe, the parasite count also increased in the Mc group (Fig. 2A).

The relative expression of the 60S ribosomal protein L18 of *T. bryosalmonae* (RPL18) gene in kidney tissues was evaluated in both single and co-infection. The peak load of *T. bryosalmonae* was recorded in the Tb group at 1 dpc (1 mpe). *T. bryosalmonae* burden decreased over time, with the Tb+

Figure 2A

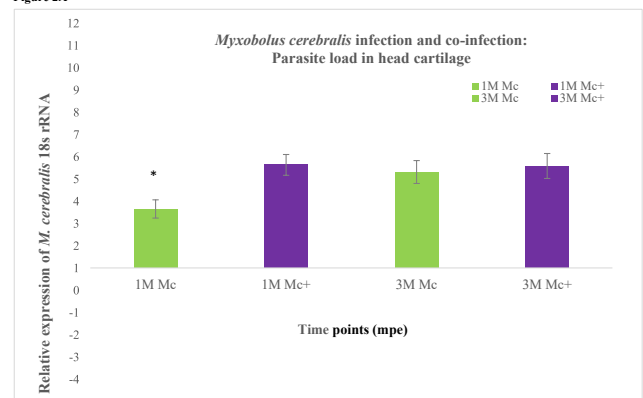


Figure 2B

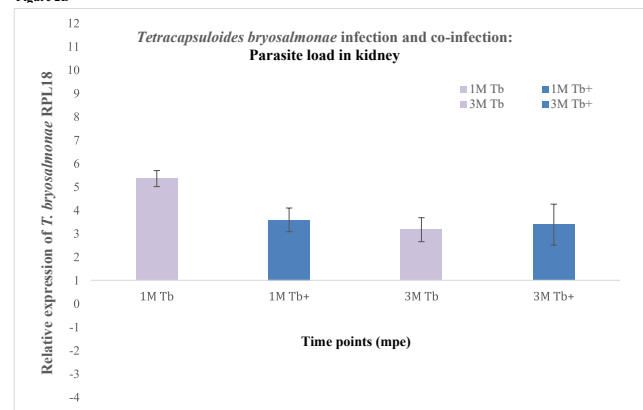


Figure 2: Parasite load in the head cartilage (1A) and kidney (1B) at 1 dpc and 2 mpc (1 and 3 mpe) after single and co-infections. Relative fold change was initially normalized to elongation factor 1 alpha and subsequently expressed as a fold change relative to expression levels of control fish. One-way analysis of variance (ANOVA) with Tukey's α -correction was used to examine the differences between the groups at each time point. The statistical differences were regarded as significant at a p -value ≤ 0.001 .

group exhibiting the lowest parasite count at 2 mpc (3 mpe) (Fig. 2B).

Proteins differentially regulated in the head cartilage

In the head cartilage, 36 rainbow trout proteins were differentially regulated between the groups. The Tb group was not included in subsequent analyses, as *T. bryosalmonae* doesn't affect the head cartilage. The relative distribution of these proteins, classified by function, is shown in Table 1. The upregulated proteins are mainly involved in signal transduction, immune response, and host protection against oxidative stress, while the downregulated ones are associated with cytoskeleton organization, protein folding, metabolism, and DNA repair.

Extracellular matrix (ECM) and cytoskeleton proteins differentially regulated in head cartilage at 1 dpc and 2 mpe (1 and 3 mpe)

Among the 36 differentially regulated proteins in the head cartilage, six were involved in extracellular matrix and cytoskeleton organization (Table 2).

At 2 mpc (3 mpe), in addition to spectrin beta, the abundance of catenin delta 1 was also induced in Mc+ fish. On the other hand, 2 of 4 downregulated extracellular proteins including actin alpha 1 and gamma-catenin were decreased in Mc and Mc+ fish. In Tb+ fish, the abundance of myosin, actin alpha 1 and the LIM zinc-binding proteins was reduced at 2 mpc (3 mpe) (Table 2). Among the decreased extracellular proteins, the abundance of gamma-catenin was extremely reduced (≤ -100) at 2 mpc (3 mpe).

Proteins differentially regulated in head cartilage involved in protein folding, transcriptional regulation and metabolism at 1 dpc and 2 mpe (1 and 3 mpe)

In our study, 15 proteins implicated in transcriptional regulation, protein folding, and metabolism were differentially regulated between the groups (Table 3).

The abundance of 13 proteins associated with protein folding, transcriptional regulation, and metabolism were decreased in Mc, Mc+, and Tb+ at 2 mpc (3 mpe). Among these proteins, the extended synaptotagmin-like protein,

Table 1: The table presents the main molecular functions of the top differentially regulated proteins in the head cartilage in rainbow trout against single and coinfection, based on annotation and protein domain characterization.

Differentially Regulated Proteins	Protein Functions	Number of proteins in Mc fish	Number of proteins in Mc+ fish	Number of proteins in Tb+ fish
Top Induced Proteins in the Head Cartilage in Infected Fish Groups	Extracellular and cytoskeletal activities (actin binding; cell adhesion)	1	2	-
	Transcriptional regulation (DNA and RNA repair)	1	1	2
	Signal transduction	3	4	4
	Immune response (complement; proteases; lectins)	-	2	4
	Host protection (oxidoreductase and thioredoxin activities)	1	1	1
	Total Number of Top Induced Proteins in the Head Cartilage in Infected Fish Groups		6	10
Top Reduced Proteins in the Head Cartilage in Infected Fish Groups	Extracellular and cytoskeletal activities (actin binding; cell adhesion)	2	2	4
	Transcriptional regulation (DNA and RNA repair)	1	1	1
	Protein folding	1	1	4
	Metabolism	3	3	4
	Signal transduction	-	-	3
	Immune response (complement; proteases; lectins)	-	2	2
Total Number of Top Reduced Proteins in the Head Cartilage in Infected Fish Groups		7	10	20

C-terminal binding protein, and peptidylprolyl isomerase showed the most significant reductions in values (≤ -100). Only two proteins, namely alpha-ketoglutarate-dependent dioxygenase and RNA-binding protein Luc7-like 1 showed increased levels.

Proteins differentially regulated in head cartilage

involved in signal transduction, immune response and host protection at 1 dpc and 2 mpc (1 and 3 mpe)

The levels of 15 proteins involved in signal transduction, immune response, and host protection were differentially regulated between the groups (Table 4). Eleven proteins, including collapsin, complement C3, and thioredoxin, were

Table 2: Differentially regulated proteins involved in cytoskeleton organisation and extracellular matrix in the head cartilage of infected fish post single and co-infection at 1M (1 mpe)/1 dpc and 3M (3 mpe)/2 mpc; M: Month; Mc and Mc+: *M. cerebralis* single and co-infection, Tb+: *T. bryosalmonae* co-infection; Significant regulation (a fold change of at least +/-2 as well as ANOVA and Tukey post-hoc p -value ≤ 0.001) is shown in red with asterisks. The fold changes greater/smaller than +/- 100 are artificial fold changes derived from division of the mean abundance value of one group by a mean abundance of 1 in the other group or vice versa, when the protein is ON/OFF regulated.

Accession	Description	Mc 3M / Mc 1M	Mc+ 1M/ Mc 1M	Mc+ 3M/ Mc 1M	Mc+ 3M/ Mc 3M	Mc+ 3M/ Mc+ 1M	Tb+ 1M/ Mc 1M	Tb+ 1M/ Mc+ 1M	Tb+ 3M/ Mc 3M	Tb+ 3M/ Mc+ 3M	Tb+ 3M/ Tb+ 1M
A0A8C7S210	Myosin	-1.7	1.2	-2	-1.2	-2.5	1.1	-1.1	-7.8*	-6.6	-14.6*
A0A8C7LQL2	Actin alpha 1 (ACTC), skeletal muscle	-2.6*	1	-2.5*	1.1	-2.5*	-1.1	-1.1	-1.2	-1.3	-2.8*
A0A8C7UWY4	Spectrin beta	3.7*	-1.3	3.2*	-1.2	4.3*	1.1	1.4	-1.2	-1.1	2.8
A0A8C7P7S7	Junction plakoglobin (gamma-catenin)	-100*	-1.1	-100*	1	-100*	1	1.2	1	1	-100*
A0A060W2D5	Catenin delta 1	2.5	-1.1	2.7	1.1	3.1*	-1.1	1	1	-1.1	2.8
A0A8K9UFU2	LIM zinc-binding domain-containing protein	-4.4	-1.6	-1.7	2.6	-1.1	-1.3	1.2	-1.9	-4.9	-6.6*

Table 3: Differentially regulated proteins involved in protein folding, metabolism, DNA and RNA repair in the head cartilage of infected fish post single and co-infection at 1M (1 mpe)/ 1 dpc and 3M (3 mpe)/2 mpc; M: Month; Mc and Mc+: *M. cerebralis* single and co-infection, Tb and Tb+: *T. bryosalmonae* single and co-infection. Significant regulation (a fold change of at least +/-2 as well as ANOVA and Tukey post-hoc p -value ≤ 0.001) is shown in red with asterisks. The fold changes greater/smaller than +/- 100 are artificial fold changes derived from division of the mean abundance value of one group by a mean abundance of 1 in the other group or vice versa, when the protein is ON/OFF regulated.

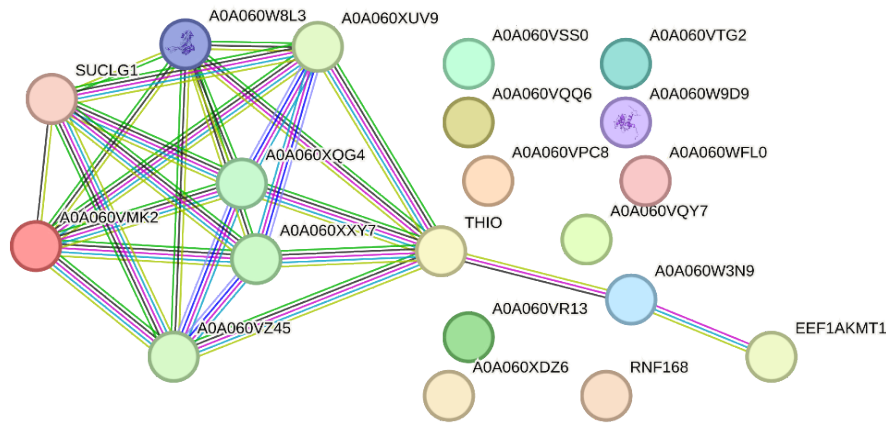
Accession	Description	Mc 3M / Mc 1M	Mc+ 1M/ Mc 1M	Mc+ 3M/ Mc 1M	Mc+ 3M/ Mc 3M	Mc+ 3M/ Mc+ 1M	Tb+ 1M/ Mc 1M	Tb+ 1M/ Mc+ 1M	Tb+ 3M / Mc 3M	Tb+ 3M/ Mc+ 3M	Tb+ 3M/ Tb+ 1M
A0A8K9USB4	Thymidine phosphorylase	-1.9	1	-1.6	1.1	-1.7	-1.1	-1.1	-1.5	-1.7	-2.6*
A0A8C7UJS8	Globin domain-containing protein	-4.7	1.2	-6	-1.3	-6.9	1	-1.1	-2.8	-2.2	-13.4*
A0A060XSW0	Globin domain-containing protein	-3.8	-1.4	-4	-1	-2.9	-1.2	1.1	-4	-3.8	-12.6*
A0A060XKZ9	Extended synaptotagmin-like	-2.3	-1	-2.2	1.1	-2.1	-1.3	-1.3	-100*	-100*	-100*
A0A060YPK0	Succinate-CoA ligase subunit beta	-10.6	2	-15.2	-1.4	-30.9*	1	-2	-2.8	-2	-31.2*
A0A8K9WV69	Histone	-22.9*	1.7	-33.9*	-1.5	-59.0*	-1.5	-2.5	1.1	1.7	-13.9*

A0A060XRV6	Globin domain-containing protein	-1.8	-1.1	-3.5	-1.9	-3.1	1.2	1.3	-4.5	-2.3	-9.5*
A0A060W8L3	Delta-1-pyrroline-5-carboxylate synthase	-1.6	1.6	-3.7	-2.3	-6.0*	-1	-1.7	1.7	3.9	1.1
A0A8C7VAK2	Ubiquitin-conjugating enzyme E2D 4	-3.7*	-1	-3.6*	1	-3.5	-1.1	-1.1	-2.2	-2.3	-7.4*
A0A8C7UNT5	C-terminal binding protein	-100*	1.3	-100*	1	-100*	1.2	-1.1	1	1	-100*
A0A8C7R074	Peptidylprolyl isomerase	-100*	1.5	-100*	1	-100*	1	-1.5	1	1	-100*
A0A8C7RVM0	Endoplasmic reticulum oxidoreductase alpha	3.7	-4.1	1.1	-3.4	4.5	-3.3	1.2	-6.0*	-1.8	2
A0A8K9XPG4	Alpha-ketoglutarate-dependent dioxygenase	2	2	1.5	-1.3	-1.3	1.3	-1.5	2.9	3.9*	4.4*
A0A8C7PLN6	Zgc:158803 (putative RNA-binding protein Luc7-like 1)	2.5*	-1.2	2.8*	1.1	3.3*	-1.4	-1.2	1.1	-1.1	3.9*
A0A8C7LSH8	Dimethylglycine dehydrogenase	-5.2*	1.1	-3.1	1.7	-3.5	1.3	1.2	1.5	-1.1	-4.7*

Table 4: Differentially regulated proteins involved in signal transduction, immune response and host protection in the head cartilage of infected fish post single and co-infection at 1M (1 mpe)/ 1 dpc and 3M (3 mpe)/2 mpc); M: Month; Mc and Mc+: *M. cerebralis* single and co-infection, Tb and Tb+: *T. bryosalmonae* single and co-infection Significant regulation (a fold change of at least +/-2 as well as ANOVA and Tukey post-hoc *p*-value ≤ 0.001) is shown in red with asterisks. The fold changes greater/smaller than +/- 100 are artificial fold changes derived from division of the mean abundance value of one group by a mean abundance of 1 in the other group or vice versa, when the protein is ON/OFF regulated.

Accession	Description	Mc 3M / Mc 1M	Mc+ 1M/ Mc 1M	Mc+ 3M/ Mc 1M	Mc+ 3M/ Mc 3M	Mc+ 3M/ Mc+ 1M	Tb+ 1M/ Mc 1M	Tb+ 3M / Mc 3M	Tb+ 1M/ Mc+ 1M	Tb+ 3M/ Mc+ 3M	Tb+ 3M/ Tb+ 1M
A0A8C7PBV1	Complement C3-like	2.4	-1.1	4.4	1.8	5.0*	1.3	1.6	1.5	-1.1	2.9
A0A8C7WGH6	Transketolase	2.6	-1.2	3.5*	1.4	4.2*	1.1	1.3	1.3	-1.1	3.1*
A0A8C7S3Z3	Proteasome subunit beta	-1.5	-1.1	-2.6*	-1.7	-2.4*	1.2	-1.6	1.3	1	-3.1*
A0A8C7TMC0	Thymus-specific serine protease	-2	-1.5	-4.6*	-2.3	-3.1	-1.1	-3	1.4	-1.3	-5.4*
A0A8C7M4S8	GOLD domain-containing protein	2.1*	1	1.4	-1.5	1.4	-1.2	1	-1.3	1.5	2.7*
A0A8K9V2M6	Acidic nuclear phosphoprotein 32	3.9*	-1.4	3.4*	-1.2	4.7*	1.1	-1.3	1.5	-1.1	2.8
C1BH85	Thioredoxin	10.6*	-1.9	5.5	-1.9	10.5*	1	-1.5	1.9	1.3	7.2*
Q8UWM6	Stress protein HSP70	1.6	1.8	1.2	-1.3	-1.4	-3.6	-1.2	-6.5*	1.1	4.8
A0A8C7UU52	Nucleoprotein TPR	-1.6	1.1	-1.5	1	-1.6	1.5	5.3*	1.4	5.1*	2.2
A0A8K9UWE7	Prosaposin	1.8	-1	1.6	-1.2	1.6	-2.4	1.2	-2.3	1.4	5.1*
A0A8C7TL27	Phosphorylase kinase	1.9	1.1	2.9	1.5	2.7	4.8*	3.8	4.4	2.4	1.5
C1BFU0	Cytochrome c oxidase subunit 5B	1.5	1	4.2*	2.9*	4.1*	1.1	2.2	1.1	-1.3	2.8*

A0A8K9XGR1	Bactericidal permeability-increasing protein	1.5	1	1.2	-1.2	1.2	-3.3	1.5	-3.5*	1.9	7.6*
A0A8K9XM33	Collapsin response mediator protein 1	7.2*	-2.9	5.4*	-1.3	15.8*	1	-2.5	3	-1.9	2.8
C0KIP4	C type lectin receptor B	2.6	1.2	6.1*	2.3	5.0*	1	3.2	-1.2	1.4	8.5*



● A0A060VMK2	TRANSKETOLASE_1 domain-containing protein. (628 aa)
● A0A060VPC8	LIM zinc-binding domain-containing protein. (337 aa)
● A0A060VQ6	Peptidylprolyl isomerase. (436 aa)
● A0A060VQ7	Proteasome subunit beta; Belongs to the peptidase T1B family. (253 aa)
● A0A060VR13	Fibronectin type-III domain-containing protein. (926 aa)
● A0A060VSS0	Myosin motor domain-containing protein; Belongs to the TRAFAC class myosin-kinesin ATPase superfamily. Myosin family. (1007 aa)
● A0A060VTG2	Lipocln_cytosolic_FA-bd_dom domain-containing protein; Belongs to the calycin superfamily. Lipocalin family. (193 aa)
● A0A060W3N9	Elongation factor 1-alpha; This protein promotes the GTP-dependent binding of aminoacyl- tRNA to the A-site of ribosomes during protein biosynthesis. (458 aa)
● A0A060W8L3	Delta-1-pyrroline-5-carboxylate synthase; In the C-terminal section; belongs to the gamma-glutamyl phosphate reductase family. (780 aa)
● A0A060W9D9	Spectrin beta chain; Belongs to the spectrin family. (2411 aa)
● A0A060WFL0	GLOBIN domain-containing protein; Belongs to the globin family. (196 aa)
● SUCLG1	Succinate-CoA ligase [ADP/GDP-forming] subunit alpha, mitochondrial; Succinyl-CoA synthetase functions in the citric acid cycle (TCA), coupling the hydrolysis of succinyl-CoA to the synthesis of either ATP or GTP and thus represents the only step of substrate-level phosphorylation in the TCA. The alpha subunit of the enzyme binds the substrates coenzyme A and phosphate, while succinate binding and specificity for either ATP or GTP is provided by different beta subunits. (356 aa)
● RNF168	E3 ubiquitin-protein ligase RNF168; E3 ubiquitin-protein ligase required for accumulation of repair proteins to sites of DNA damage. Acts with UBE2N/UBC13 to amplify the RNF8-dependent histone ubiquitination. Recruited to sites of DNA damage at double-strand breaks (DSBs) by binding to ubiquitinated histone H2A and ubiquitinates histone H2A and H2AX, leading to amplify the RNF8-dependent H2A ubiquitination and promoting the formation of 'Lys-63'-linked ubiquitin conjugates. This leads to concentrate ubiquitinated histones H2A and H2AX at DNA lesions to the threshold required for recrui [...] (509 aa)
● A0A060XDZ6	Phosphorylase b kinase regulatory subunit; Phosphorylase b kinase catalyzes the phosphorylation of serine in certain substrates, including troponin I. Belongs to the phosphorylase b kinase regulatory chain family. (213 aa)
● THIO	Thioredoxin; Belongs to the thioredoxin family. (108 aa)

Figure 3: String protein-protein interaction network of the main differentially regulated head cartilage proteins. In this network, nodes are proteins, lines represent the predicted functional associations, and the number of lines represents the strength of predicted function interactions between proteins. All scores rank from 0 to 1, with 1 being the highest possible confidence. The predicted interactions have a score of more than 0.5, which indicates a 50% confidence score.

significantly induced between Mc, Mc+, and Tb+ at 2 mpc (3 mpe).

On the other hand, the abundance of hsp70, thymus-specific serine protease, and proteasome subunit alpha was reduced in the Mc+ group at 2 mpc (3 mpe).

Protein-protein interaction networks of head cartilage proteins

The STRING analysis provided important information on the protein-protein interactions, pathways, and biological processes enriched in the head cartilage (the target organ of *M. cerebralis*) in rainbow trout (Fig. 3 and 4).

Carbon metabolism, citrate, biosynthesis of amino acids, metabolic pathways, the pentose phosphate pathway, and one

carbon pool by folate are among the pathways that have been identified in the cranial cartilage (Fig. 4).

Based on protein domain characterization of the annotated proteins that were significantly modulated in the head cartilage, various molecular functions appear to be triggered by *M. cerebralis* (Fig. 4). The molecular functions of the head cartilage proteins assigned by KEGG analysis include oxidoreductase, thioredoxin-disulfide reductase, and thiamine pyrophosphate binding, which serves as a cofactor for many translocases. The proteins implicated in protein folding and transcriptional control demonstrate various functions, including mRNA regulatory element binding, translation repression, amino acid binding, and mRNA 5' untranslated region binding.

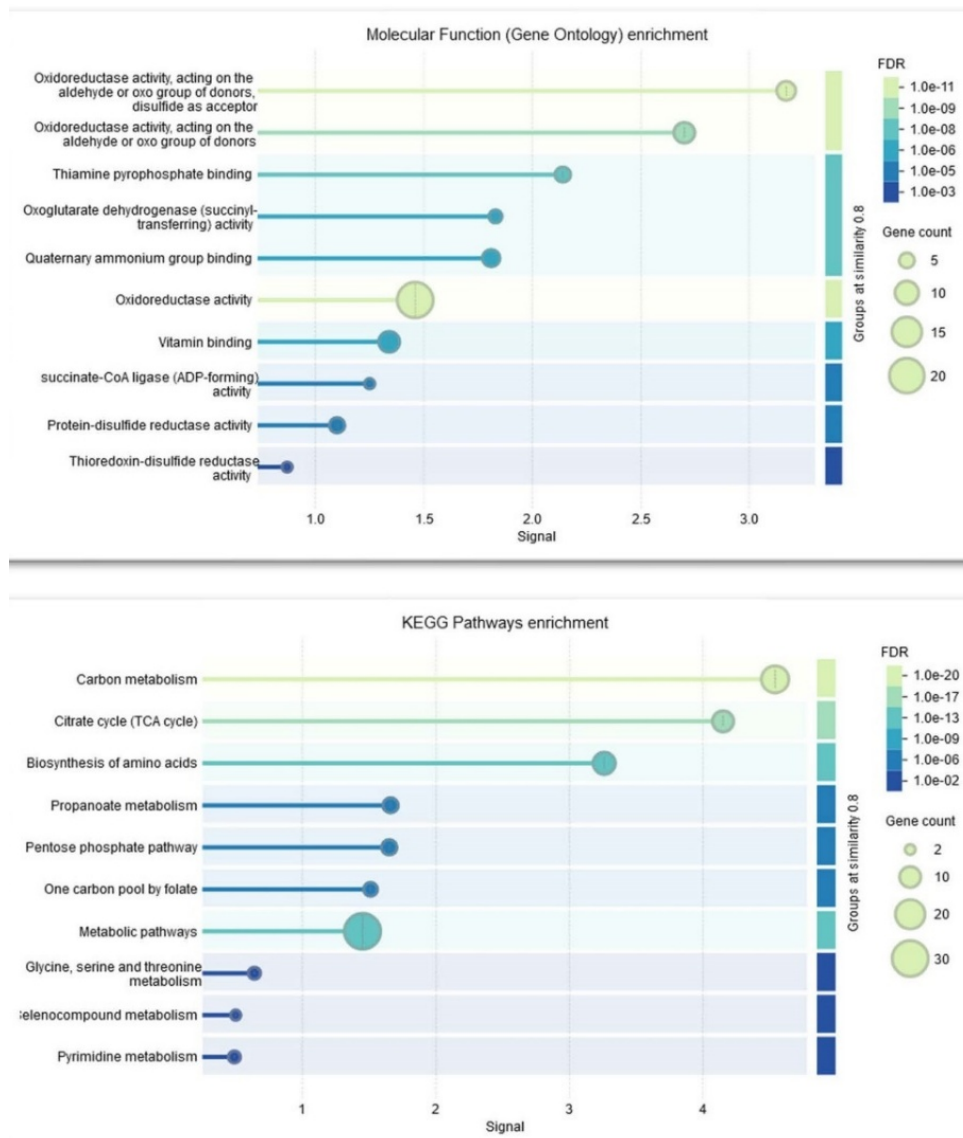


Figure 4: The diagram shows that the metabolism pathways and antioxidative stress response are among the top KEGG pathways and the main molecular function of differentially regulated proteins in the head cartilage based on annotation and protein domain characterization.

Table 5: The table presents the main molecular functions of the top differentially regulated proteins in the kidney in rainbow trout against single and coinfection, based on annotation and protein domain characterization.

Category	Molecular Functions	Number of proteins in Mc fish	Number of proteins in Mc+ fish	Number of proteins in Tb+ fish
Top Induced Proteins in the Kidney in Infected Fish Groups	Extracellular and cytoskeletal activities (actin binding; cell adhesion)	-	1	1
	Transcriptional regulation (DNA and RNA repair)	-	4	6
	Immune response (complement; proteases; lectins)	1	4	17
	Host protection (oxidoreductase and thioredoxin activities)	-	1	1
Total Number of Top Induced Proteins in the Kidney in Infected Fish Groups		1	10	25
Top Reduced Proteins in the Kidney in Infected Fish Groups	Extracellular and cytoskeletal activities (actin binding, cell adhesion)	5	7	7
	Transcriptional regulation (DNA and RNA repair)	1	-	-
	Metabolism	5	6	6
	Immune response (complement; proteases; lectins)	1	2	3
Total Number of Top Reduced Proteins in the Kidney in Infected Fish Groups		12	15	16

Table 6: Top differentially regulated proteins involved in cytoskeleton organisation and extracellular matrix in the kidney of infected fish post single and co-infection at 1M (1 mpe)/ 1 dpc and 3M (3 mpe)/2 mpc; M: Month; Mc and Mc+: *M. cerebralis* single and co-infection, Tb and Tb+: *T. bryosalmonae* single and co-infection; Asterisks show significant fold changes. Significant regulation (a fold change of at least +/-2 as well as ANOVA and Tukey post-hoc *p*-value ≤ 0.001) is shown in red with asterisks. The fold changes greater/smaller than +/- 100 are artificial fold changes derived from division of the mean abundance value of one group by a mean abundance of 1 in the other group or vice versa, when the protein is ON/OFF regulated.

Accession	Description	Mc 3M / Mc 1M	Mc+ 1M/ Mc 1M	Mc+ 3M/ Mc 1M	Mc+ 3M/ Mc 3M	Mc+ 3M/ Mc+ 1M	Tb+ 1M/ Mc 1M	Tb+ 3M / Mc 3M	Tb+ 1M/ Mc+ 1M	Tb+ 3M/ Mc+ 3M	Tb+ 3M/ Tb+ 1M
Q90W76	Type II keratin E1	-3.9	-2.1	-11.0*	-2.8	-5.1	-1.3	-3	1.6	-1	-8.9
Q90W75	Type II keratin E2	-5.3	-1.7	-5.9	-1.1	-3.5	-1.2	-5.7	1.4	-5.1	-25.2*
A0A060Y5W1	Myosin motor	-58.1*	-1.8	-89.2*	-1.5	-49.9*	-1.5	-1.7	1.2	-1.1	-64.3*
A0A8C7T9E0	Myosin motor	-37.3*	-1.9	-29.2*	1.3	-15.4	-1.8	-1.6	1.1	-2	-32.3*
A0A8C7NJH5	Myosin light chain	-56.9	-1.4	-85.6*	-1.5	-62.1*	-1.3	-2.9	1.1	-1.9	-100*
A0A8C7SMF8	Myosin, heavy chain 10	-7.7*	-1.8	-12.6*	-1.6	-6.9*	-1.1	-100*	1.7	-100*	-100*
A0A8C7PCS9	Myosin IG	2.1	1.1	3.8*	1.8	3.3*	1.1	1.9	-1	1.1	3.7*
A0A8K9Y6I6	PDZ and LIM	-100*	1	-100*	1	-100*	1.2	1	1.2	1	-100*
A0A8C7T270	Plexin D1	-72.9*	-1.6	-100*	-2.5	-1.6	-100*	-6.6	1	-2.6	-100*

Citation: Mona Saleh, Karin Hummel, Sarah Schlosser, Ebrahim Razzazi-Fazeli, Jerri L Bartholomew, Christopher J. Secombes, Mansour El-Matbouli. Quantitative Proteomic Profiling of Stress and Immunological Responses in Target Organs Reveals How Myxozoan Parasites Determine the Outcome of Rainbow Trout Co-Infections. Archives of Microbiology and Immunology. 9 (2026): 57-79.

Proteins differentially regulated in the kidney

In the kidney, 618 rainbow trout proteins were differentially regulated between the groups. These include 504 upregulated proteins that are mainly involved in signal transduction, host immunity, and protection against oxidative damage and oxidative stress. On the other hand, the abundance of 114 proteins mainly associated with extracellular matrix (ECM) and cytoskeleton organization was downregulated. The proteomic analysis of the kidney of infected fish identified numerous proteins implicated in diverse functions related to the host's response during infection (Table 5). Among these are several proteins involved in signal transduction (protein kinase C and serine kinase), host immunity (complement C3, immunoglobulin, and MHC II), transcription (transcription factor A), tissue repair, and protection against oxidative damage and stress (thioredoxin).

Proteins differentially regulated in kidney involved in extracellular matrix (ECM) and cytoskeleton organisation

The levels of many ECM and cytoskeletal structure proteins were decreased (Table 6). The proteins exhibiting the most pronounced reductions in levels comprise type II keratin (three members) and various myosin proteins (eleven members). Five downregulated myosins had markedly diminished levels (≤ -100), while one myosin protein (myosin IG) was considerably elevated in the Mc+ and Tb+ fish at 2 mpc (3 mpe). The level of PDZ and LIM proteins (2 members) was significantly downregulated (≤ -100) in the kidneys of Mc-infected fish and in the co-infected Mc+ and Tb+ fish. Plexin D1 was significantly downregulated (≤ -100) in Tb+ fish at 2 mpc (3 mpe).

Table 7: Differentially regulated proteins involved in metabolism, DNA and RNA repair and protein folding in the kidney of infected fish post single and co-infection at 1M (1 mpe)/ 1 dpc and 3M (3 mpe)/2 mpc; M: Month; Mc and Mc+: *M. cerebralis* single and co-infection, Tb and Tb+: *T. bryosalmonae* single and co-infection; Asterisks show significant fold changes. Significant regulation (a fold change of at least +/-2 as well as ANOVA and Tukey post-hoc *p*-value ≤ 0.001) is shown in red with asterisks. The fold changes greater/smaller than +/- 100 are artificial fold changes derived from division of the mean abundance value of one group by a mean abundance of 1 in the other group or vice versa, when the protein is ON/OFF regulated.

Accession	Description	Mc 3M / Mc 1M	Mc+ 1M/ Mc 1M	Mc+ 3M/ Mc 1M	Mc+ 3M/ Mc 3M	Mc+ 3M/ Mc+ 1M	Tb+ 1M/ Mc 1M	Tb+ 3M / Mc 3M	Tb+ 1M/ Mc+ 1M	Tb+ 3M/ Mc+ 3M	Tb+ 3M/ Tb+ 1M
A0A8K9XP47	Thymidine phosphorylase	1	1	1	1	1	1	100*	1	100*	100*
A0A060YGG5	serine--tRNA ligase	3.1	1	5.6*	1.8	5.5*	1.3	3.7	1.3	2.1	8.6*
A0A8C7Q9G9	leucine--tRNA ligase	1.7	-1.1	1.9	1.1	2.2	-1.5	1.1	-1.3	-1.1	2.7*
A0A8K9XBL9	cysteine--tRNA ligase	1.3	1.1	-1.3	3.9	4.7	5	8.5*	1.4	2.2	7.1*
A0A060YXE3	E3 ubiquitin-protein ligase TRIM21-like	1.1	1.1	3.1	2.8	2.8	-1.2	3.9	-1.3	1.4	5.2*
A0A060VY96	KH domain-containing protein	-100*	4	2.3	100*	-1.7	1.9	100*	-2.1	1.9	-2.2
A0A8C7STY9	DNA replication licensing factor MCM2	2.7	-1.4	4	1.5	5.6*	1.2	1.2	1.6	-1.2	2.8
A0A8C7SX25	DNA replication licensing factor MCM2	1.6	-1.6	2.2	1.4	3.6*	-1.2	1.7	1.3	1.3	3.4*
A0A8C7UMZ0	Calsequestrin	-88.6*	-1.6	-100*	-2.1	-100*	-1.5	-2.1	1.1	1	-100*
A0A060X5F1	Parvalbumin	-54.0*	-1.8	-100*	-2.1	-64.1*	-1.6	-1.5	1.1	1.4	-50.5*
E0WDA3	Parvalbumin	-18.2*	-1.6	-30.0*	-1.6	-19.1*	-1.1	-2.3	1.4	-1.4	-38.5*
A0A060XWA9	Parvalbumin	-14.1*	-1.5	-24.3*	-1.7	-15.8*	-1.2	-1.8	1.2	-1	-19.9*
A0A060YVV4	Parvalbumin	-79.1*	-1.6	-100*	-2.6	-100*	-1.5	-1.6	1.1	1.7	-100*
A0A060WZV7	Troponin C type 2	-60.1	-1.4	-100*	-2.1	-86.8	-1.7	-4.2	-1.2	-2	-100*

Proteins differentially regulated in kidney involved in metabolism, DNA and RNA repair and protein synthesis

The levels of several proteins involved in protein synthesis, DNA and RNA repair, and metabolism were differentially regulated between the groups (Table 7).

The abundance of thymidine phosphorylase was highly increased (≥ 100) in the Mc+ and Tb+ fish at 2 mpc (3 mpe). In addition, the abundance of E3 ubiquitin-protein ligase TRIM21-like and the levels of various other tRNA ligases linked to RNA repair, such as tyrosine-tRNA ligase, methionine-tRNA ligase, and cysteine-tRNA ligase, were mostly elevated in Tb+ fish at 2 mpc (3 mpe). Likewise,

the abundance of multiple proteins involved in RNA transcription and DNA replication, including the KH domain-containing protein and the DNA replication licensing factor MCM2, was upregulated in Mc+ and Tb+ fish at 2 mpc (3 mpe). The quantity of KH domain-containing protein and DNA replication licensing factor MCM2 (two members) was elevated in Mc+ and Tb+ fish at 2 mpc (3 mpe). On the other hand, the abundance of vitellogenin and 6-phosphofructo-2-kinase/fructose-2,6-biphosphatase domain-containing protein, which are involved in lipid and carbohydrate metabolism and transport, was extremely decreased in the kidney of Tb+ fish at 2 mpc (3 mpe). The level of palmitoyl transferase involved in lipid metabolism was also extremely reduced in the Mc+ fish as well as in the co-infected fish

Table 8: Differentially regulated proteins involved in signal transduction, immune response and host protection in the kidney of infected fish post single and co-infection at 1M (1 mpe)/ 1 dpc and 3M (3 mpe)/2 mpc; M: Month; Mc and Mc+: *M. cerebralis* single and co-infection; Tb and Tb+: *T. bryosalmonae* single and co-infection; Asterisks show significant fold changes. Significant regulation (a fold change of at least +/-2 as well as ANOVA and Tukey post-hoc p -value ≤ 0.001) is shown in red with asterisks. The fold changes greater/smaller than +/- 100 are artificial fold changes derived from division of the mean abundance value of one group by a mean abundance of 1 in the other group or vice versa, when the protein is ON/OFF regulated.

Accession	Description	Mc 3M / Mc 1M	Mc+ 1M/ Mc 1M	Mc+ 3M/ Mc 1M	Mc+ 3M/ Mc 3M	Mc+ 3M/ Mc+ 1M	Tb+ 1M/ Mc 1M	Tb+ 3M / Mc 3M	Tb+ 1M/ Mc+ 1M	Tb+ 3M/ Mc+ 3M	Tb+ 3M/ Tb+ 1M
A0A8C7PBV1	Complement C3-lik	4.6*	1.1	7.7*	1.7	7.2*	2.1	1.7	1.9	1	3.9*
A0A8K9WTM6	Complement factor H	3.4	3.1	8.5	2.5	2.7	-4.5	3.3	-14	1.3	51*
Q9GJ12	MHC class II beta-chain	1	1	100*	100*	100*	1	1	1	-100*	1
A0A8K9Y483	Ig-like domain-containing protein	1	1	1	1	1	1	100*	1	100*	100*
A0A8C7SYI3	Ig-like domain-containing protein	1.8	1.3	-100*	1.1	1.5	2	3.6	-100*	3.2	100*
A0A8C7PZE5	Ig-like domain-containing protein	2.9	1.7	5	1.7	3	1	3.6	-1.6	2.1	10.4*
A0A8C7R4F5	Ig-like domain-containing protein	1.5	1.2	2.7	1.8	2.3	-1.2	7.5	-1.4	4.3	14.0*
A0A859IQK1	Cathepsin L-like	-1.8	-1.1	1.7	3.2	1.5	2.7	6	-3	1.9	8.7*
A0A060YXS6	Cathepsin B	1.4	1.3	2.3	1.6	1.7	-1.7	3.1	-2.2	1.9	7.2*
A0A8K9XXD3	26S proteasome regulatory subunit 6B	1.8	1.2	2.6	1.5	2.1	-1.1	1.7	-1.3	1.2	3.3*
A0A060XJ24	Proteasome subunit alpha	1.8	1.7	3.3	1.8	1.9	1.2	2.5	-1.5	1.4	3.8*
A0A060YAL5	Proteasome subunit alpha	-1.8	1.1	2.9	1.6	2.6	-1.4	1.8	-1.5	1.1	4.4*

A0A8C7REH1	Proteasome subunit beta	1.7	1.2	4.1	2.4	3.6	-1.1	3	-1.3	1.3	5.8*
A0A8K9UMM3	Proteasome activator complex	1.6	1.3	4.1	2.5	3.2	-1.3	4	-1.6	1.6	8.2*
A0A060WJ19	Proteasome activator complex	1.3	1.4	3.9*	3	2.8	-1.1	4.4*	-1.5	1.5	6.3*
A0A060YXB8	Proteasome assembly chaperone 2	3.8	1.8	7.1*	1.8	3.8	-2.4	-1.4	-4.5	-2.5	6.7*
A0A8C7VMW9	SERPIN domain-containing protein	1	1	1	1	1	1	100*	1	100*	100*
A0A060XM71	Serpin H1	-44.3*	-1.8	-94.8*	-2.1	-53.8*	-1.7	-1.6	1	1.3	-43.2*
A0A8C7UVL2	Thioredoxin	-2.4	1.3	2.2	5.1*	1.7	1.9	13.7*	15	2.7	3

Table 9: Differentially regulated myxozoan proteins in the kidney of infected fish post single and co-infection at 1M (1 mpe)/ 1 dpc and 3M (3 mpe)/2 mpc; M: Month; Mc and Mc+: *M. cerebralis* single and co-infection, Tb and Tb+: *T. bryosalmonae* single and co-infection; Asterisks show significant fold changes. Significant regulation (a fold change of at least +/-2 as well as ANOVA and Tukey post-hoc *p*-value ≤ 0.001) is shown in red with asterisks.

Accession	Description	Mc 3M / Mc 1M	Mc+ 1M/ Mc 1M	Mc+ 3M/ Mc 1M	Mc+ 3M/ Mc 3M	Mc+ 3M/ Mc+ 1M	Tb+ 1M/ Mc 1M	Tb+ 3M / Mc 3M	Tb+ 1M/ Mc+ 1M	Tb+ 3M/ Mc+ 3M	Tb+ 3M/ Tb+ 1M
A0A859IQF9	Hsp 70 cognate <i>Tetracapsuloides bryosalmonae</i>	-1.3	2.1	23.2*	29.5*	10.8	3.8	45.7*	1.8	1.6	9.3
A0A859IQP1	Hsp 90-alpha <i>Tetracapsuloides bryosalmonae</i>	1.3	1.1	8.4*	6.5	7.8	1.3	7.9*	1.2	1.2	7.7
A0A859IQC5	Hsp 70 Bip-like protein <i>Tetracapsuloides bryosalmonae</i>	-1.9	-1.4	20.8	40.1	29.6	1.4	83.4*	1.9	2.1	31.8
Q26045	Antigen PKX101 proliferative kidney organism	-1.4	1.1	4.9	7	4.7	1.2	11.4*	1.2	1.6	6.4
A0A0C2IU88	Elongation factor 2 <i>Thelephanelus kitauei</i>	1.9	-1.1	2.3	1.2	2.8	-1.3	1.6	-1.1	1.3	8.7*
A0A6G3MGA4	Heat shock 70 kDa protein F, mitochondrial <i>Henneguya salminicola</i>	1.3	1	2.1	1.6	2	-1.1	2.2	-1.2	1.4	3.2*
A0A859IQK1	Cathepsin L-like <i>Tetracapsuloides bryosalmonae</i>	-1.8	1.1	1.7	3.2	1.5	-2.6	6	-3	1.9	8.7*
I6ZY10	Elongation factor 2 <i>Myxidium coryphaenoideum</i>	1.9	-1.1	2.4	1.3	2.7	-1.2	1.6	-1.1	1.2	3.7*

Mc+ and Tb+ at 2 mpc (3 mpe). In addition, the abundance of several proteins, including calsequestrin, parvalbumin, and troponin C, was enormously downregulated (≤ -100) in the Tb+ fish at 1 dpc (1 mpe) and in the Mc, Mc+, and Tb+ fish at 2 mpc (3 mpe).

Proteins differentially regulated in kidney involved in signal transduction, immune response and host protection

Among the broadly expanded and induced proteins, we identified multiple complement C3 members, MHC II, and thioredoxin (Table 8). The Ig-like domain-containing proteins (5 members) were differentially regulated between the groups and showed high abundance values (≥ 100), primarily in Tb+ fish.

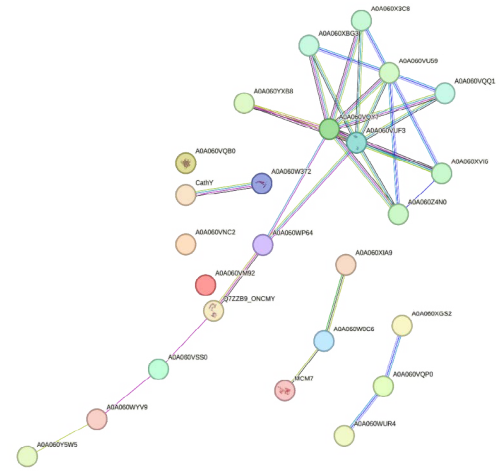
Several proteins involved in protein degradation and proteasome assembly, such as proteases including cathepsin (2 members), proteasome subunit alpha (3 members), proteasome subunit beta, proteasome activator complex subunit 2 (2 members), 26S proteasome regulatory subunit 6B, and the proteasome assembly chaperone 2, were upregulated in the co-infection groups Mc+ and Tb+ at 2 mpc (3 mpe). Multiple kinases, including protein kinase C and serine kinase, which are involved in signal transduction, were also differentially regulated between the groups at 1 dpc and 2 mpc (1 and 3 mpe). In Mc+ fish, the abundance of 4 lectins was upregulated, and one of these, namely the c-type lectin, was extremely induced (≥ 100). Multiple serpins were induced, showing the highest upregulation (≥ 100) in Tb+ fish. One serpin domain-containing protein was unchanged, and the collagen chaperone Serpin H1, also known as hsp47, was extremely downregulated in Tb+ fish at 1 dpc (1 mpe) and in Mc, Mc+, and Tb+ fish at 2 mpc (3 mpe).

Differentially regulated myxozoan proteins

In the head cartilage, two *M. cerebralis* proteins, the beta-actin (Q818C8) and the elongation factor 2 (E3U3Z2), were differentially regulated, showing minimal changes between the groups, mainly in the Tb+ group. In kidney, 8 myxozoan proteins, including actin, myosin, hsp70, hsp70 Bip-like (immunoglobulin-binding protein), hsp90, antigen PKX101, and cathepsin L-like, were differentially regulated between the groups (Table 9). Proteins involved in protein degradation, parasite development, and virulence, such as hsp70, hsp70 Bip, hsp90, the antigen PKX101, and cathepsin, were upregulated in Mc+ and Tb+ groups at 2 mpc (3 mpe). Among these, the most highly induced proteins are hsp70 (≥ 45) and hsp70 Bip (≥ 83 -fold), which show increased abundance levels in the Tb+ group at 2 mpc (3 mpe).

The protein–protein interaction network of kidney proteins

The STRING analysis provided important information



● AQA060VM92	Palmitoyltransferase; Belongs to the DHHC palmitoyltransferase family. (678 aa)
● AQA060VNC2	Vitellogenin domain-containing protein. (1378 aa)
● AQA060VQB0	FERM domain-containing protein. (1570 aa)
● AQA060VQP0	Ig-like domain-containing protein. (309 aa)
● AQA060VQY7	Proteasome subunit beta; Belongs to the peptidase T1B family. (253 aa)
● AQA060VSS0	Myosin motor domain-containing protein; Belongs to the TRAFAC class myosin-kinesin ATPase superfamily. Myosin family. (1007 aa)
● AQA060VUF3	Proteasome subunit alpha type. (282 aa)
● AQA060W0C6	DNA topoisomerase 2; Control of topological states of DNA by transient breakage and subsequent rejoining of DNA strands. Topoisomerase II makes double-strand breaks. (1559 aa)
● AQA060W372	SERPIN domain-containing protein; Belongs to the serpin family. (420 aa)
● AQA060WP64	Calsequestrin; Calsequestrin is a high-capacity, moderate affinity, calcium-binding protein and thus acts as an internal calcium store in muscle. (419 aa)
● MCM7	DNA replication licensing factor MCM7; Acts as component of the mcm2-7 complex (mcm complex) which is the putative replicative helicase essential for once per cell cycle DNA replication initiation and elongation in eukaryotic cells. The active ATPase sites in the mcm2-7 ring are formed through the interaction surfaces of two neighboring subunits such that a critical structure of a conserved arginine finger motif is provided in trans relative to the ATP-binding site of the Walker A box of the adjacent subunit. The six ATPase active sites, however, are likely to contribute differential [...] (727 aa)
● AQA060WYV9	Uncharacterized protein; Belongs to the parvalbumin family. (108 aa)
● AQA060XIA9	Tyrosine-tRNA ligase. (480 aa)
● CathY	Cathepsin Y; Belongs to the peptidase C1 family. (290 aa)
● QZZB9_UNCMY	Troponin C. (161 aa)

Figure 5: String protein-protein interaction network of the main differentially regulated kidney proteins. In this network, nodes are proteins, lines represent the predicted functional associations, and the number of lines represents the strength of predicted function interactions between proteins. All scores rank from 0 to 1, with 1 being the highest possible confidence. The predicted interactions have a score of more than 0.5, which indicates a 50% confidence score.

on the protein-protein interactions, pathways, and biological processes enriched in the kidney (the target organ of *T. bryosalmonae*) in rainbow trout (Fig. 5 and 6).

The biological processes associated with the observed proteomic changes in the kidney in rainbow trout are mainly involved in host protection against oxidative stress, DNA and protein synthesis, and metabolism. The top identified pathways in the kidney included the proteasome, glutathione metabolism, and arginine and proline metabolism (Fig. 6).

The gene ontology analysis of the significantly modulated proteins in the kidney identified various molecular functions likely triggered by *T. bryosalmonae*, including endopeptidase activity, NF-kappaB binding, and proteasome binding (Fig. 6).

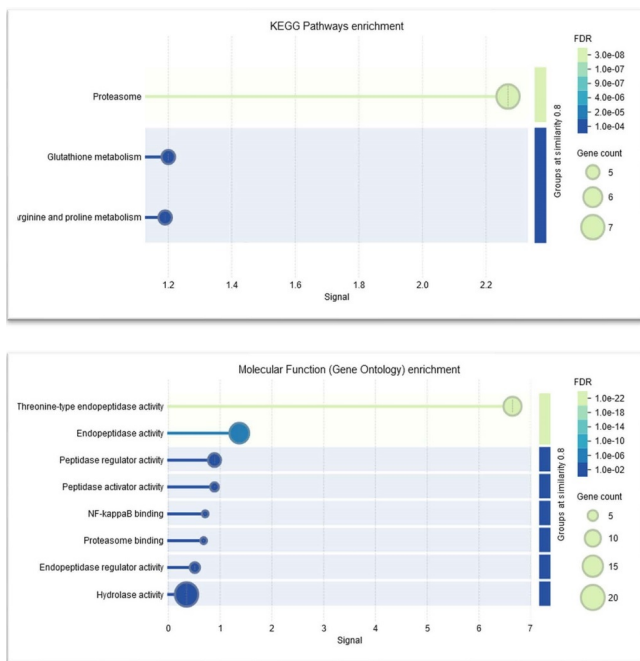


Figure 6: The diagram shows that the proteasome and different metabolism pathways and various peptidase/protease activities are among the top KEGG pathways and the main molecular function of differentially regulated proteins in the kidney based on annotation and protein domain characterisation.

Discussion

Recently, the proteomic profiles of the rainbow trout portals of entry for *M. cerebralis* and *T. bryosalmonae* in single and co-infections revealed novel molecular traits of the host immune responses and fish myxozoan interactions [8]. However, proteome modulation and protein changes at the target organs of the two parasites, the head cartilage (target of *M. cerebralis*) and the kidney (target of *T. bryosalmonae*), are not well explored. Hence, in the current study, we aimed to explore the proteomic changes induced by these two parasites at their target organs during *M. cerebralis* and *T. bryosalmonae* single and co-infection in rainbow trout. This proteomic study highlights traits of the host-parasite interactions and the immune response of rainbow trout to co-infections with the two different myxozoan parasites at their target organs and potentially facilitates development of effective interventions and therapeutic strategies to help control these diseases.

Myxobolus cerebralis and *Tetracapsuloides bryosalmonae* parasite burden

In the head cartilage, the parasite load increased in the co-infected group Mc+ group at 1 dpc and 2 mpc (1 and 3 mpe) as compared to the single infected Mc group. The increased *M. cerebralis* load in the head cartilage implies that the fish were unable to maintain proper tissue homeostasis,

immunity, or limit parasite load during WD as previously reported [10, 11, 13, 29, 8, 14, 15]. Conversely, the parasite count decreased in the Tb+ group as compared to the Tb group in the kidney. The reduced parasite load in the kidney implies that the fish were able to constrain the development and growth of the parasite, likely by triggering balanced host protection mechanisms and maintaining tissue homeostasis, corresponding to previous studies [26, 29, 23]. These findings emphasize that the primary infection determines the outcome of a subsequent co-infection in rainbow trout.

Extracellular matrix and cytoskeletal proteins

In the head cartilage, catenin delta 1 was one of significantly upregulated in the head cartilage in Mc+ fish at 2 mpc (3 mpe). This protein is associated with extracellular matrix, focal adhesion, and cadherin-catenin complex formation. It regulates the NF-κB transcription factor and has a critical role in neuronal development and chromatin biology in zebrafish [46]. Delta catenin has different binding partners, which indicates that it may play different roles in different cellular subcompartments [47]. On the other hand, the abundance of gamma-catenin with structural and signaling roles was extremely decreased in Mc and the co-infected fish Mc+ and Tb+ at 2 mpc (3 mpe), suggesting that the two catenin proteins may have different roles in head cartilage tissue in rainbow trout. Actin alpha 1 was also downregulated in Mc, Mc+, and Tb+ infected fish at 2 mpc (3 mpe). In addition, the abundance of myosin and LIM zinc binding with structural and signal transduction roles was decreased in Tb+ fish at 2 mpc (3 mpe). Such proteins are associated with signal transduction, tissue repair, and regeneration in fish and after parasitic infections [48, 49, 50, 51, 52, 53]. Here, the decreased abundance of several extracellular and cytoskeletal proteins in Mc, Mc+, and Tb+ fish at 2 mpc (3 mpe) mirrors the inability of the host fish to compensate for tissue damage due to parasite evasion and increased parasite load.

In the kidney, the levels of 114 proteins associated with ECM and cytoskeleton organization were mainly downregulated, including type II keratin (3 members) and multiple myosin proteins (11 members). Keratin II is a cytoskeletal protein with a crucial role in protecting cells from mechanical and non-mechanical damage [54]. The keratin II from fish mucus has pore-forming activities [55]. Furthermore, keratin II turnover depends on the ubiquitin–proteasome pathway and is modulated by cell injury [56]. In olive flounder gills, keratin II was downregulated in response to *Streptococcus parauberis* infection or VHSV [57]. Likewise, in the current study, the rainbow trout keratin II proteins were downregulated in Tb+ fish, likely a myxozoan strategy to evade host immune responses. Five of the downregulated myosins were extremely downregulated (≤ -100) in the Mc+ and Tb+ fish at 2 mpc (3 mpe). These

cytoskeletal proteins are associated with cell structure, tissue repair, and regeneration in fish and are modulated during parasitic infections [49, 50, 52]. Only myosin IG was upregulated in the Mc⁺ and Tb⁺ fish at 2 mpc (3 mpe), suggesting a different role for this protein during myxozoan co-infections. PDZ and LIM domain proteins are involved in the organization and maintenance of the Z-lines in striated muscle in Atlantic salmon [48]. The downregulation of the PDZ-LIM proteins after single and co-infections reflects a possible impairment in the organization and maintenance of kidney tissues during myxozoan infections. Plexin D1 is a cellular receptor that modulates the cytoskeleton and cell adhesion and regulates cellular migration [58, 59]. This protein also exhibited marked downregulation (≤ 100) in Mc, Mc⁺, and Tb⁺ fish. Here, the decreased abundance of several extracellular and cytoskeletal proteins in Mc, Mc⁺, and Tb⁺ fish reflects the inability of the host fish to cope with tissue damage and adverse effects caused by the parasites after infection.

Protein folding, metabolism, DNA and RNA repair proteins

In the head cartilage, several proteins involved in transcription and protein folding were extremely reduced. Peptidylprolylisomerase protein was extremely downregulated (≤ -100) in Mc, Mc⁺, and Tb⁺ fish at 2 mpc (3 mpe). This protein has roles in protein folding and was differentially regulated in the gills of infected zebrafish in response to *Aeromonas hydrophila* [60]. In addition, the abundance of the extended synaptotagmin was also extremely reduced (≤ -100 -fold) in Tb⁺ fish at 2 mpc (3 mpe). The protein is involved in lipid binding and transport [61, 62]. On the other hand, two proteins, alpha-ketoglutarate-dependent dioxygenase and RNA-binding protein Luc7-like 1, involved in RNA and DNA repair, showed increased levels, likely to compensate for the adverse effects after exposure to *M. cerebralis*. In a previous study, the deletion of alpha-ketoglutarate-dependent dioxygenase caused considerable defects in epiboly during embryo gastrulation in zebrafish [63]. Here, the abundance of alpha-ketoglutarate-dependent dioxygenase and RNA-binding protein Luc7-like 1 was increased after exposure to *M. cerebralis* infected rainbow trout, likely to repair tissue destruction and adverse events due to parasite development in head cartilage tissues. The identified pathways of the head cartilage proteins include carbon metabolism (protein synthesis), the citrate cycle (TCA cycle), biosynthesis of amino acids, one carbon pool of folate (biosynthesis, amino acid homeostasis, epigenetic maintenance, and redox defense), the pentose phosphate pathway (DNA and RNA synthesis), and metabolic pathways. Synaptotagmin-like, the C-terminal binding protein, and peptidylprolyl isomerase proteins, which are involved in protein folding and metabolism, were highly reduced (≤ -100). The decreased levels of proteins involved

in protein folding and metabolism indicate the inability of the host fish to cope with the adverse effects of the increased parasite load. The increased *M. cerebralis* load in the head cartilage shows that the fish are unable to limit parasite burden during WD (Fig. 2A). This observation agrees with similar findings previously reported [13, 29, 8, 14, 15].

In kidney tissues, in addition to thymidine phosphorylase, the abundance of several ligases, including E3 ubiquitin-protein ligase and multiple tRNA ligases including tyrosine-tRNA ligase, methionine-tRNA ligase, and cysteine-tRNA ligase, was mostly upregulated in Tb⁺ fish at 2 mpc (3 mpe). Likewise, the abundance of multiple proteins involved in RNA transcription and DNA replication, including the KH domain-containing protein and the DNA replication licensing factor MCM2, was upregulated in Mc⁺ and Tb⁺ fish at 2 mpc (3 mpe). The increased abundance of these proteins was likely associated with RNA transcription and DNA and RNA repair to compensate for tissue damage and adverse effects triggered by the parasite. During parasitic infection with *Cryptocaryon irritans* in yellow croaker, similar proteins, including E3 ubiquitin ligase, were induced [64]. Conversely, several proteins involved in muscle contraction and calcium transport, such as calsequestrin, parvalbumin, and troponin C, were strikingly downregulated (≤ -100) in the Tb⁺ fish at 1 dpc (1 mpe) as well as in the two co-infection groups, Mc⁺, and Tb⁺, at 2 mpc (3 mpe). The contraction of the smooth muscles surrounding the collecting tubule can increase intratubular pressure, affecting the glomerular filtration rate, and may also affect the transport activity of tubule cells (Tsuneki et al., 1984). We thus propose that the suppression of these proteins negatively impacts the glomerular filtration rate and the transport activity of tubule cells during PKD, thereby affecting the release of *T. bryosalmonae* spores and hindering the completion of the parasite life cycle in rainbow trout. However, functional analysis studies are needed to reveal the exact role of these proteins in rainbow trout during PKD.

Signal transduction, immune response and host protection proteins

Multiple proteins involved in signal transduction, immune response, and host protection were differentially regulated in the head cartilage between the groups. These comprise 11 proteins, such as collapsing response mediator 1, complement C3, lectin, and thioredoxin, which were significantly induced in Mc, Mc⁺, and Tb⁺ at 2 mpc (3 mpe). Collapsin response mediator proteins (CRMPs) are a family of cytosolic phosphoproteins that play important roles during neural development in zebrafish [65]. CRMP1 is a key downstream mediator of the Semaphorin-3A signal transduction pathway implicated in axon guidance and neuronal migration [66]. CRMP1 was induced in Mc, Mc⁺, and Tb⁺ fish, likely to

enhance signal transduction and activate molecules involved in immune defense and protection against damage caused during parasite development and replication. In our previous study, we observed that various immune defense molecules involved in host immunity and protection against oxidative stress were induced during co-infections by the two parasites (Saleh 2024). On the other hand, the levels of the proteasome subunit alpha, hsp70, and thymus-specific serine protease were reduced, which may indicate the inability of fish to keep proper tissue homeostasis and failure to cope with tissue damage caused by the parasite.

The abundance of multiple complement related proteins, including complement C3, was induced in the kidney of Mc, Mc+, and Tb+ fish at 2 mpc (3 mpe). In addition, the complement factor H protein was highly increased in Tb+ fish at 2 mpc (3 mpe). In our previous study, the abundance of the complement factor H protein was increased in caudal fin tissues in the co-infection groups Mc+ and Tb+ [8]. Complement factor H can bind to various ligands, protecting host cells from damage and thereby contributing to tissue hemostasis and the immune response of rainbow trout against myxozoan co-infections at the entry sites by impeding the complement system [67]. This regulator can inhibit the alternative pathway of the complement system and prevent the synthesis of C3 convertase, thereby hindering complement activation [68]. The complement factor H protein was able to bind to pathogenic bacteria and maintain a proper homeostasis in the host and pathogen [67]. The increased abundance in the co-infection groups implies that the complement factor H protein contributes to tissue homeostasis and immunity of rainbow trout against myxozoan co-infections.

The B cell signature proteins MHC II and several Ig-like domain containing proteins showed elevated abundance up to ≥ 100 in the kidney of the co-infection groups, especially in the Mc+ fish (after co-infection with *T. bryosalmonae*) at 2 mpc (3 mpe). This agrees with previous studies, which have shown that *M. cerebralis* and *T. bryosalmonae* can activate B cells during infections [16, 23]. In addition, the B-cell markers Ig-like domain and MHC II were induced (≥ 100) in the gills in the co-infected fish [8]. Further, proteins involved in protein degradation and proteasome assembly, including proteases such as cathepsin, 26S proteasome regulatory subunit 6B, proteasome subunit alpha, proteasome subunit beta, proteasome activator complex subunit 2, and the proteasome assembly chaperone 2, were induced, showing high elevation levels in the co-infection groups Mc+ and Tb+ at 2 mpc (3 mpe). The proteasome and metabolism of several amino acids were the main pathways modulated within the rainbow trout kidney proteins. Likewise, during parasitic infection with *Ichthyophthirius multifiliis*, the proteasome and metabolism pathways were the most highly represented in the head kidney of rainbow trout [69]. This is likely

because when fish are overwhelmed by stress or infection, the excessive or misfolded proteins must be processed and degraded by proteolytic activities in the proteasome [70, 69]. Serpins are serine protease inhibitors that impede tissue damage, excessive proteolysis, and complement-dependent cell lysis [71]. In the current study, several serpins were induced in kidney tissues, likely aimed at protection against tissue damage and excessive proteolysis triggered by *T. bryosalmonae*. On the other hand, serpin H1 showed reduced levels in Mc, Mc+, and Tb+ fish at 2 mpc (3 mpe) and was extremely reduced in Tb+ fish at 1 dpc (1 mpe). Serpin H1 can influence bone growth and skeletal patterning and is believed to exert its function through the organization of collagen proteins in the extracellular matrix [72]. In addition, serpin H1 is likely involved in wound healing and structural repair of damaged tissues in Atlantic salmon after infection with sea lice and in response to *Moritella viscosa* [73, 74]. The extreme reduced abundance of serpin H1 in Tb+ fish at 1 dpc (1 mpe) suggests a reduced collagen organization in the extracellular matrix after a subsequent co-infection with *M. cerebralis*. Only one serpin remained unchanged, possibly interfering with *T. bryosalmonae*, as previously reported. The lack of modulation (up- or downregulation) of only one serpin can be likely attributed to *T. bryosalmonae* due to its interaction and interference with this serpin, inhibiting its binding to proteases, which is essential for serpin modulation, as observed during infections with VHSV [71]. Clearly, functional investigations are required to explain whether and how *T. bryosalmonae* interferes with serpin, preventing its modulation.

Collectively, in Tb+ and Mc+ fish, among several signal transduction and immune response proteins, multiple proteins involved in signal transduction (protein kinase C and serine kinase), host immunity (complement C3, immunoglobulin, and MHC II), transcription (transcription factor A), tissue repair, and protection against oxidative damage and stress (thioredoxin) were highly induced in the kidney (Fig. 7). In the head cartilage of the Mc+ fish, we observed decreased levels of the proteins involved in cytoskeleton organization and metabolism, and increased parasite count. This fact shows that *M. cerebralis* renders its host unable to cope with tissue damage triggered during parasite development and growth, which increases the fish's vulnerability to subsequent co-infections. In the kidney of the Tb+ fish, the upregulated proteins are associated with host immunity and DNA and RNA repair, signifying that *T. bryosalmonae* primes host immunity, enabling a proper tissue homeostasis and a balanced immune response. Unexpectedly, the kidney with a high number of differentially regulated proteins (618) showed fewer enriched GO terms than the cartilage with low numbers (37). This is likely because the kidney is showing controlled responses with several proteins of similar function, aiming at maintaining a balanced response and tissue homeostasis.

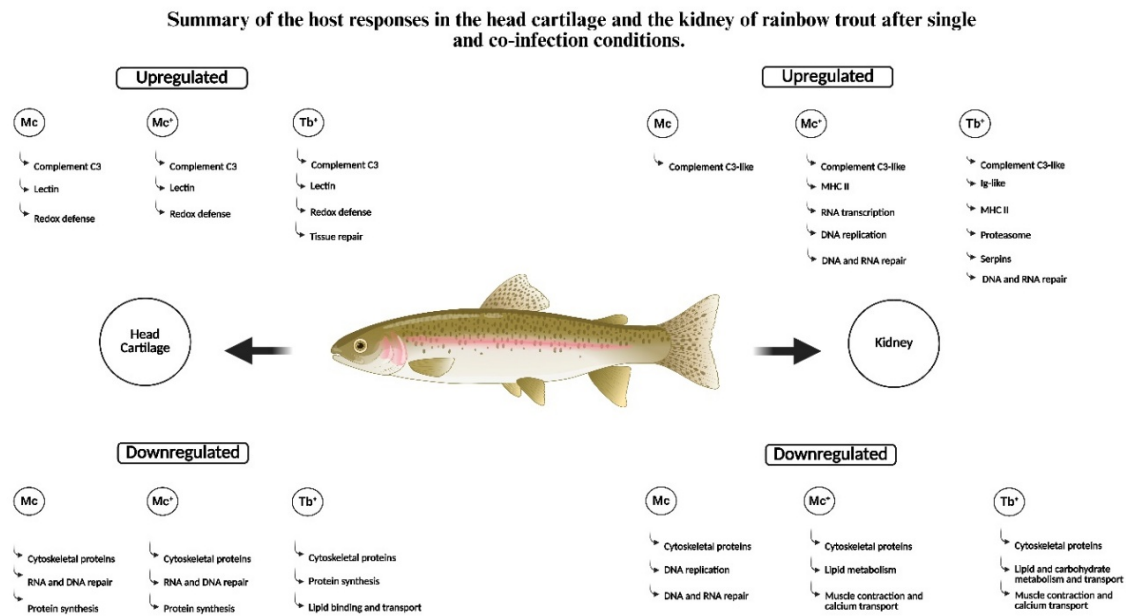


Figure 7: Summary of the host responses in the head cartilage and the kidney of rainbow trout showing top shared responses and organ specific signatures after single and co-infections. The figure was created with BioRender.com.

Common proteins differentially expressed between both organs include complement C3, different kinases and thioredoxin. Kinases are known to activate various immune signaling pathways, including the c-type lectin pathway. Lectins are important for sensing and degrading dead cells and play a pivotal role in host defense against pathogens and for tissue homeostasis [75]. The marked upregulation (≥ 100) of c-type lectin in Mc+ fish suggests that the host is responding in a way that aims to limit parasite replication and development, cope with accompanied tissue damage, and maintain proper tissue homeostasis following subsequent co-infection with *M. cerebralis*.

Parasite Proteins

In addition to the modulated host proteins, eight myxozoan proteins, including hsp70, hsp70 Bip-like, hsp90, antigen PKX101, and cathepsin L-like, were identified in the fish kidney. These proteins likely have a role in parasite development, virulence, and growth. The expression of the heat shock proteins hsp60, hsp70, and hsp90 *T. bryosalmonae* homologues was increased in Bryozoa and fish, implying a potential role in parasite survival, temperature-driven development, and host invasion [76]. Hsp70, in particular, has roles in cell structure, cell regulation, protein assembly, folding, and translocation during parasitic infestations in fish [77, 78, 8]. In our previous proteome study, four myxozoan proteins were significantly increased in Mc+ fish gills [8]. As a vaccine adjuvant, hsp70 provides high protection against the fish parasite *C. irritans* in orange spotted grouper [79]. Hence, it is important to investigate functionally whether and how hsp70 could exert such protection in rainbow trout. The

binding immunoglobulin protein (BiP) of the hsp70 family chaperone is localized in the ER lumen. As a highly conserved molecular chaperone, hsp70-BiP assists in a wide range of folding processes. It is implicated in directing misfolded proteins into ERDM for degradation and is involved in protein translocation [80]. The abundance of the myxozoan hsp70 Bip-like protein was highly elevated (≥ 83 -fold) in the kidney in the Tb+ fish kidney at 2 mpc (3 mpe). This molecule is likely used by the parasite to keep proteostasis to counteract host responses and favor its survival within the host. The precise role of hsp70-BiP during myxozoan infections deserves further functional investigations.

The increase of critical myxozoan virulence proteins, such as hsp70, hsp70 Bip-like, hsp90, antigen PKX101, and cathepsin L, in the kidney in Mc+ and Tb+ fish at 2 mpc (3 mpe) underscores the involvement of such molecules in potential invasion/evasion strategies during myxozoan infections as previously suggested [8, 76]. The heightened prevalence of the virulence genes in the kidney at 2 mpc (3 mpe) represents a parasitic approach to sustain homeostasis and mitigate the host's immune responses during co-infections. However, functional experiments are essential to elucidate and confirm the specific role of these proteins and to further understand how myxozoans influence the result of co-infection in rainbow trout.

Conclusion

The biological processes, signalling pathways, and molecular functions of the differentially regulated proteins revealed that many of them were involved in the immune

response, DNA and RNA repair, and host protection. Considering that the fish kidney (the main target organ of *T. bryosalmonae*) is a major hematopoietic organ playing a vital role in protection against pathogens, that the number of identified and quantified proteins was much higher here than in the head cartilage was expected. Most of the highly upregulated proteins in the kidney are associated with host immunity and DNA and RNA repair, indicating that *T. bryosalmonae* primes host immunity, maintains tissue homeostasis, and allows the host to mount a balanced response aimed at coping with tissue damage and adverse effects caused by the parasite in an attempt to limit tissue destruction and parasite growth. Alternatively, in the head cartilage, most of the proteins involved in cytoskeleton organization and tissue repair and metabolism were extremely downregulated, and there was a limited upregulation of the signaling and immune response proteins, implying that *M. cerebralis* triggers excessive tissue destruction and damage, leaving its host unable to maintain tissue homeostasis during parasite development and growth, increasing fish vulnerability to subsequent co-infections.

It is important to note that calsequestrin, parvalbumin, and troponin C, which are involved in muscle contraction and calcium transport, were extremely downregulated in the kidney in infected fish. These proteins likely contribute to the transport activity of tubule cells during PKD, which may influence the development of intraluminal sporogonic stages of *T. bryosalmonae* in the renal tubular lumen of rainbow trout, impacting the release of viable *T. bryosalmonae* spores and hindering the completion of the parasite life cycle in rainbow trout and its transmission to the bryozoan invertebrate host. However, functional studies are needed to elucidate and confirm the precise role that these proteins might play, contributing to the fact that rainbow trout is considered a dead-end host fish for *T. bryosalmonae*. Indeed, future transcriptomic and genomic studies, as well as functional analysis, will help understand the basis of the interactions between fish and myxozoans, specifically during WD and PKD single and co-infections.

Overall, the current study provides key information on how myxozoan parasites distinctly modulate immune signaling pathways and immune response proteins, enhancing our understanding of host myxozoan interactions in single and co-infection consequences, potentially facilitating the development of effective interventions and therapeutic strategies for WD and PKD management in salmonid aquaculture. Future transcriptomic and genomic studies as well as functional analysis can help reveal important interactions between myxozoans within host salmonid fish, specifically during WD and PKD single and co-infections.

Data availability statement

The mass spectrometry proteomics data have been deposited to the ProteomeXchange Consortium via the

PRIDE [1] partner repository with the dataset identifier PXD077587 and 10.6019/PXD077587.

Author contributions

MS and ME conceived and designed the study. MS performed the experiments. MS, KH, and SS analyzed the data. MS wrote the manuscript. ER, JB, CJS and ME revised the manuscript. All authors read and approved the final manuscript.

Funding: This study was fully funded by the Austrian Science Fund (FWF) project no. P32340.

Acknowledgements

This research was supported using resources of the VetCore Facility (Proteomics) of the University of Veterinary Medicine Vienna. The authors would like to thank Reza Ghanei-Motlagh for helping during the experiments and analysis. Naveed Akram is also thanked for helping with the BioRender figures.

Conflict of interest

The authors declare that the research was conducted in the absence of any commercial or financial relationships that could be construed as a potential conflict of interest.

References

- Hofer B. Über die drehkrankheit der regenbogenforelle. Allg. Fisch Ztg. 28 (1903): 7–8.
- Hoffman GL. Myxobolus cerebralis, a worldwide cause of salmonid whirling disease. J. Aquat. Anim. Health 2 (1990): 30–37.
- Wolf K, Markiw ME. Biology contravenes taxonomy in the Myxozoa: new discoveries show alternation of invertebrate and vertebrate hosts. Science 225 (1984): 1449–52.
- Hedrick RP, El-Matbouli M, Atkinson MA, et al. Whirling disease: re-emergence among wild trout. Immunol. Rev 166 (1998): 365–76.
- Schisler GJ, Bergersen EP, Walker PG. Effects of multiple stressors on morbidity and mortality of fingerling rainbow trout infected with Myxobolus cerebralis. Trans. Am. Fish Soc 129 (2000): 859–865.
- Wahli T, Bernet D, Segner H, et al. Role of altitude and water temperature as regulating factors for the geographical distribution of Tetracapsuloides bryosalmonae infected fishes in Switzerland. J. Fish Biol 73 (2008): 2184–2197.
- Akram N, El-Matbouli M, Saleh M. The immune response to the Myxozoan parasite Myxobolus cerebralis in salmonids: A review on whirling disease. Int. J Mol Sci 24 (2023): 17392.

8. Saleh M, Hummel K, Schlosser S, et al. The myxozoans *Myxobolus cerebralis* and *Tetracapsuloides bryosalmonae* modulate rainbow trout immune responses: quantitative shotgun proteomics at the portals of entry after single and co-infections. *Front. Cell Infect. Microbiol* 13 (2024): 1369615.
9. Rucker U, El-Matbouli M. Sequence analysis of OmNramp alpha and quantitative expression of Nramp homologues in different trout strains after infection with *Myxobolus cerebralis*. *Dis. Aquat. Org* 76 (2007): 223-30.
10. Severin VI, El-Matbouli M. Relative quantification of immune-regulatory genes in two rainbow trout strains, *Oncorhynchus mykiss*, after exposure to *Myxobolus cerebralis*, the causative agent of whirling disease. *Parasitol. Res* 101 (2007): 1019-27.
11. Severin VI, Soliman H, El-Matbouli M. Expression of immune-regulatory genes, arginase-2 and inducible nitric oxide synthase (iNOS), in two rainbow trout (*Oncorhynchus mykiss*) strains following exposure to *Myxobolus cerebralis*. *Parasitol Res* 106 (2010): 325-34.
12. Baerwald MR, Welsh AB, Hedrick RP, et al. Discovery of genes implicated in whirling disease infection and resistance in rainbow trout using genome-wide expression profiling. *BMC Genomics* 9 (2008): 37.
13. Baerwald MR. Temporal expression patterns of rainbow trout immune-related genes in response to *Myxobolus cerebralis* exposure. *Fish Shellfish Immunol* 35965 (2013): 71.
14. Saleh M, Friedl A, Srivastava M, et al. STAT3/SOCS3 axis contributes to the outcome of salmonid whirling disease. *PLoS One* 15 (2020a): e0234479.
15. Saleh M, Friedl A, Srivastava M, et al. Modulation of local and systemic immune responses in brown trout (*Salmo trutta*) following exposure to *Myxobolus cerebralis*. *Fish Shellfish Immunol* 1050-4648 (2020b): 30619-7.
16. Saleh M, Montero R, Kumar G, et al. Kinetics of local and systemic immune cell responses in whirling disease infection and resistance in rainbow trout. *Parasit. Vectors* 12 (2019a): 249.
17. Canning EU, Curry A, Feist SW, et al. A new class and order of myxozoans to accommodate parasites of bryozoans with ultrastructural observations on *Tetracapsula bryosalmonae* (PKX organism). *J Eukaryot Microbiol* 47 (2000): 456-68.
18. Morris DJ, Adams A. Transmission of *Tetracapsuloides bryosalmonae* (Myxozoa: Malacosporea), the causative organism of salmonid proliferative kidney disease, to the freshwater bryozoan *Fredericella sultana*. *Parasitology* 133 (2006): 701-9.
19. Grabner DS, El-Matbouli M. *Tetracapsuloides bryosalmonae* (Myxozoa: Malacosporea) portal of entry into the fish host. *Dis. Aquat. Org* 90 (2010): 199-208.
20. Gorgoglione B, Kotob MH, El-Matbouli M. Migrating zooids allow the dispersal of *Fredericella sultana* (Bryozoa) to escape from unfavourable conditions and further spreading of *Tetracapsuloides bryosalmonae*. *J. Invertebr. Pathol* 140 (2016a): 97-102.
21. Okamura B, Hartikainen H, Schmidt-Posthaus H, et al. Life cycle complexity, environmental change and the emerging status of salmonid proliferative kidney disease. *Freshwater Biol* 56 (2011): 735-53.
22. Gorgoglione B, Kotob MH, Unfer G, et al. First proliferative kidney disease outbreak in Austria, linking to the aetiology of black trout syndrome threatening autochthonous trout populations. *Dis. Aquat. Org* 119 (2016b): 117-128.
23. Bailey C, Holland JW, Secombes, CJ, et al. A portrait of the immune response to proliferative kidney disease (PKD) in rainbow trout. *Parasit. Immunol* 42 (2020): e12730.
24. Abd-Elfattah A, Kumar G, Soliman H, et al. Persistence of *Tetracapsuloides bryosalmonae* (Myxozoa) in chronically infected brown trout *Salmo trutta*. *Dis. Aquat. Org* 111 (2014): 41-9.
25. Abd-Elfattah A, El-Matbouli M, Kumar G. Structural integrity and viability of *Fredericella sultana* statoblasts infected with *Tetracapsuloides bryosalmonae* (Myxozoa) under diverse treatment conditions. *Vet Res* 48 (2017): 19.
26. Gorgoglione B, Wang T, Secombes CJ, et al. Immune gene expression profiling of proliferative kidney disease in rainbow trout *Oncorhynchus mykiss* reveals a dominance of anti-inflammatory, antibody and T helper cell-like activities *Vet Res* 44 (2013): 55.
27. Okamura B, Gruhl A, Bartholomew JL. An introduction to Myxozoan evolution, ecology and development. In: Okamura B, Gruhl A, Bartholomew JL (eds) *Myxozoan evolution, ecology and development*. Springer, Heidelberg (2015): 1-20.
28. Gay M, Okamura B, De Kinkelin P. Evidence that infectious stages of *Tetracapsula bryosalmonae* for rainbow trout *Oncorhynchus mykiss* are present throughout the year. *Dis. Aquat. Org* 46 (2001): 31-40.
29. Kotob MH, Kumar G, Saleh M, et al. Differential modulation of host immune genes in the kidney and cranium of the rainbow trout (*Oncorhynchus mykiss*)

- in response to *Tetracapsuloides bryosalmonae* and *Myxobolus cerebralis* co-infections. *Parasit. Vectors* 30 (2018): 326.
30. Sitjà-Bobadilla A, Schmidt-Posthaus H, Wahli T, et al. Fish immune responses to myxozoa. In: Okamura B, Gruhl A, Bartholomew J (Eds.) *Myxozoan Evolution, Ecology and Development*. Springer International Publishing, Switzerland (2015).
 31. Holzer AS, Piazzon MC, Barrett D, et al. To react or not to react: The dilemma of fish immune systems facing myxozoan infections. *Front. Immunol* 12 (2021): 734238.
 32. Holzer AS, Sommerville C, Wootten R. Molecular studies on the seasonal occurrence and development of five myxozoans in farmed *Salmo trutta* L. *Parasitology* 132 (2006): 193-205.
 33. Manrique WG, Figueiredo MAP, de Andrade Belo MA, et al. *Myxobolus* sp. and *Heneguya* sp. (Cnidaria: Myxobolidae) natural co-infection in the kidney of *Piaractus mesopotamicus* (Characiformes: Serrasalminidae). *Parasitol. Res* 116 (2017): 2853-2860.
 34. Alama-Bermejo G, Hernández-Orts JS, García-Varela M, et al. Diversity of myxozoans (Cnidaria) infecting Neotropical fishes in southern Mexico. *Sci. Rep* 13 (2023): 12106.
 35. Kotob MH, Gorgoglione B, Kumar G, et al. The impact of *Tetracapsuloides bryosalmonae* and *Myxobolus cerebralis* co-infections on pathology in rainbow trout. *Parasit. Vectors* 10 (2017): 442.
 36. El-Matbouli M, Mattes M, Soliman H. Susceptibility of whirling disease (WD) resistance and WD susceptible strains of rainbow trout *Oncorhynchus mykiss* to *Tetracapsuloides bryosalmonae*, *Yersinia ruckeri* and viral hemorrhagic septicemia virus. *Aquaculture* 288 (2009): 299-304.
 37. El-Matbouli M, Hoffmann RW, Mandok C. Light and electron microscopic observations on the route of the triactinomyxon-sporoplasm of *Myxobolus cerebralis* from epidermis into rainbow trout cartilage. *J Fish Biol* 46 (1995): 919-35.
 38. Kumar G, Abd-Elfattah A, Saleh M, et al. Fate of *Tetracapsuloides bryosalmonae* (Myxozoa) after infection of brown trout (*Salmo trutta*) and rainbow trout (*Oncorhynchus mykiss*). *Dis. Aquat. Org* 107 (2018): 9-18.
 39. Anacker R, Ordal E, et al. Studies on the myxobacterium *Chondrococcus columnaris*. I. Serological typing. *J. Bacteriol* 78 (1959): 25-32.
 40. Manual of Diagnostic Tests for Aquatic Animals Diseases of Fish: General Information (2021):
 41. Kelley GO, Zagmutt-Vergara FJ, Leutenegger CM, et al. Identification of a serine protease gene expressed by *Myxobolus cerebralis* during development in rainbow trout *Oncorhynchus mykiss*. *Dis. Aquat. Organ* 59 (2004): 235-48.
 42. Deutsch EW, Bandeira N, Perez-Riverol Y, et al. The ProteomeXchange Consortium at 10 years: 2023 update. *Nucl. Acids Res* 51 (2023): D1539-D1548.
 43. Perez-Riverol Y, Bai J, Bandla C, et al. The PRIDE database resources in 2022: A hub for mass spectrometry-based proteomics evidences. *Nucl. Acids Res* 50 (2022): D543-D552.
 44. Perez-Riverol Y, Xu QW, Wang R, et al. PRIDE Inspector Toolsuite: moving towards a universal visualization tool for proteomics data standard formats and quality assessment of ProteomeXchange datasets. *Mol. Cell Proteomics* 15 (2016): 305-17.
 45. Szklarczyk D, Morris JH, Cook H, et al. The STRING database in 2017: quality-controlled protein-protein association networks, made broadly accessible. *Nucl. Acids Res* 45 (2017): 362-68.
 46. Turner TN, Sharma K, Oh EC, et al. Loss of δ -catenin function in severe autism. *Nature*. 520 (2015): 51-6.
 47. He Y, Ki H, Kim H, et al. δ -Catenin interacts with LEF-1 and negatively regulates its transcriptional activity. *Cell Biol. Int* 39 (2015): 954-61.
 48. Andersen Ø, Østbye TK, Gabestad I, et al. Molecular characterization of a PDZ-LIM protein in Atlantic salmon (*Salmo salar*): a fish ortholog of the α -actinin-associated LIM-protein (ALP). *J Musc Res Cell Motil* 25 (2004): 61-68.
 49. Hasebe T, Kajita M, Fujimoto K, et al. Expression profiles of the duplicated matrix metalloproteinase-9 genes suggest their different roles in apoptosis of larval intestinal epithelial cells during *Xenopus laevis* metamorphosis. *Dev. Dyn* 236 (2007): 2338-2345.
 50. Camarata T, Snyder D, Schwend T, et al. Pdlim7 is required for maintenance of the mesenchymal/epidermal Fgf signaling feedback loop during zebrafish pectoral fin development. *BMC Dev Biol* 10 (2010):104.
 51. Encinas P, Rodriguez-Milla MA, Novoa B, et al. Zebrafish fin immune responses during high mortality infections with viral haemorrhagic septicaemia rhabdovirus. A proteomic and transcriptomic approach. *BMC Genomics* 11 (2010):518.
 52. Saleh M, Kumar G, Abdel-Baki AA, et al. Quantitative

- shotgun proteomics distinguishes wound-healing biomarker signatures in common carp skin mucus in response to *Ichthyophthirius multifiliis*. *Vet. Res.* 20 (2018): 37.
53. Saleh M, Kumar G, Abdel-Baki AS, et al. Quantitative proteomic profiling of immune responses to *Ichthyophthirius multifiliis* in common carp skin mucus. *Fish Shellfish Immunol.* 84 (2019b): 834-842.
54. Jacob JT, Coulombe PA, Kwan R, et al. Types I and II keratin intermediate filaments. *Cold Spring Harb. Perspect. Biol* 10 (2018): a018275.
55. Molle V, Campagna S, Bessin Y, et al. First evidence of the pore-forming properties of a keratin from skin mucus of rainbow trout (*Oncorhynchus mykiss*, formerly *Salmo gairdneri*). *Biochem J* 411 (2008): 33-40.
56. Ku NO, Omary MB. Keratins turn over by ubiquitination in a phosphorylation modulated fashion. *J. Cell Biol* 149 (2000): 547-552.
57. Lee AR, Kim H, Jeon KY, et al. Differential proteome profile of gill and spleen in three pathogen-infected *Paralichthys olivaceus*. *Genes Genomics* 43 (2021): 701-712.
58. Emerson SE, Stergas HR, Bupp-Chickering SO, et al. Shootin-1 is required for nervous system development in zebrafish. *Dev. Dyn* 249 (2020): 1285-1295.
59. Britto DD, He J, Misa JP, et al. Plexin D1 negatively regulates zebrafish lymphatic development. *Development* 149 (2022): dev200560.
60. Lü A, Hu X, Wang Y, et al. iTRAQ analysis of gill proteins from the zebrafish (*Danio rerio*) infected with *Aeromonas hydrophila*. *Fish Shellfish Immunol* 36 (2014): 229-39.
61. Idevall-Hagren O, Lü A, Xie B, et al. Triggered Ca²⁺ influx is required for extended synaptotagmin 1-induced ER-plasma membrane tethering. *EMBO J* 34 (2015): 2291-305.
62. Wen H, Linhoff MW, McGinley MJ, et al. Distinct roles for two synaptotagmin isoforms in synchronous and asynchronous transmitter release at zebrafish neuromuscular junction. *Proc. Natl. Acad. Sci. USA* 107 (2010): 13906-11.
63. Sun Q, Liu X, Gong B, et al. Alkbh4 and Atrn act maternally to regulate zebrafish epiboly. *Int. J. Biol. Sci* 13 (2017):1051-1066.
64. Zhang DL, Han F, Yu DH, et al. Characterization of E3 ubiquitin ligase neuregulin receptor degradation protein-1 (*Nrdp1*) in the large yellow croaker (*Larimichthys crocea*) and its immune responses to *Cryptocaryon irritans*. *Gene* 10 (2015): 556.
65. Jayasena CS, Trinh LA, Bronner M. Live imaging of endogenous collapsin response mediator protein-1 expression at subcellular resolution during zebrafish nervous system development. *Gene Expr. Patterns* 11 (2011): 395-400.
66. Yamashita N, Morita A, Uchida Y, et al. Regulation of spine development by semaphorin3A through cyclin-dependent kinase 5 phosphorylation of collapsin response mediator protein 1. *J Neurosci* 27 (2007): 12546-12554.
67. Wei X, Wu Z, Zhang T, et al. Functional characterization of complement factor H in host defense against bacterial pathogen in Nile tilapia (*Oreochromis niloticus*). *Fish Shellfish Immunol* 129 (2022): 114-126.
68. Du Clos TW, Mold C. Complement and complement deficiencies. *Clin. Immunol* 20 (2008): 305-325.
69. Roh H, Kim N, Lee Y, et al. Dual-organ transcriptomic analysis of rainbow trout infected with *Ichthyophthirius multifiliis* through co-expression and machine learning. *Front. Immunol* 12 (2021): 677730.
70. Martin S, Blaney S, Bowman A, et al. Ubiquitin-proteasome-dependent proteolysis in rainbow trout (*Oncorhynchus Mykiss*): Effect of food deprivation. *Pflügers Archiv* 445 (2002): 257-66.
71. Estepa A, Coll J. Inhibition of SERPINE1 reduces rhabdoviral infections in zebrafish. *Fish Shellfish Immunol* 47 (2015): 264-70.
72. Bhadra J, Iovine MK. Hsp47 mediates Cx43-dependent skeletal growth and patterning in the regenerating fin. *Mech. Dev* 138 (2015): 364-374.
73. Umasuthan N, Xue X, Caballero-Solares A, et al. Transcriptomic profiling in fins of Atlantic salmon parasitized with sea lice: Evidence for an early imbalance between chalmus-induced immunomodulation and the host's defense response. *Int. J. Mol. Sci* 21 (2020): 2417.
74. Eslamloo K, Kumar S, Xue X, et al. Global gene expression responses of Atlantic salmon skin to *Moritella viscosa*. *Sci. Rep* 12 (2022): 4622.
75. Kong W, Ding G, Cheng G, et al. Mucosal immune responses to *Ichthyophthirius multifiliis* in the ocular mucosa of rainbow trout (*Oncorhynchus mykiss*, Walbaum), an ancient teleost fish. *Mar. Life Sci. Technol.* 31 (2023): 266-279.
76. Faber M, Shaw S, Yoon S, et al. Comparative transcriptomics and host-specific parasite gene expression profiles inform on drivers of proliferative kidney disease. *Sci Rep* 11 (2021): 2149.

77. Abernathy J, Xu DH, Peatman E, et al. Gene expression profiling of a fish parasite *Ichthyophthirius multifiliis*: Insights into development and senescence-associated avirulence. *Comp. Biochem. Phy. D.* 6 (2011): 382–392.
78. Saleh M, Abdel-Baki AS, Dkhil MA, et al. Proteins of the ciliated protozoan parasite *Ichthyophthirius multifiliis* identified in common carp skin mucus. *Pathogens* 10 (2021): 790.
79. Josepriya TA, Chien KH, Lin HY, et al. Immobilization antigen vaccine adjuvanted by parasitic heat shock protein 70C confers high protection in fish against cryptosporidiosis. *Fish Shellfish Immunol* 45 (2015): 517-27.
80. Wang J, Lee J, Liem D, et al. HSPA5 Gene encoding Hsp70 chaperone BiP in the endoplasmic reticulum. *Gene* 30 (2017): 14-23.
81. Bailey C, Strepparava N, Ros A, et al. It's a hard knock life for some: Heterogeneity in infection life history of salmonids influences parasite disease outcomes. *J. Anim. Ecol* 90 (2021): 2573-2593.
82. Benjamini Y, Hochberg Y. Controlling the false discovery rate: A practical and powerful approach to multiple testing. *J. Royal Statist. Soc. Series B (Methodological)* 57 (1995): 289–300.
83. Gutiérrez AM, Sotillo J, Schlosser S, et al. Towards understanding non-infectious growth-rate retardation in growing pigs. *Proteomes* 7 (2019): 31.
84. Livak KJ, Schmittgen TD. Analysis of relative gene expression data using real-time quantitative PCR and the 2(-Delta Delta C(T)) Method. *Methods* 25 (2001): 402-8.
85. Ramires M, Hummel K, Hatfaludi T, et al. Comparative surfaceome analysis of clonal *Histomonas meleagridis* strains with different pathogenicity reveals strain-dependent profiles. *Microorganisms* 10 (2022): 1884.
86. R Core Team. R: A Language and Environment for Statistical Computing. R Foundation for Statistical Computing, Vienna (2021).
87. Tsuneki K, Kobayashi H, Pang PK. Electron-microscopic study of innervation of smooth muscle cells surrounding collecting tubules of the fish kidney. *Cell Tissue Res* 238 (1984): 307-12.
88. Wiśniewski JR, Zougman A, Nagaraj N, et al. Universal sample preparation method for proteome analysis. *Nat Methods* 6 (2009): 359-62.
89. Wiśniewski JR. Quantitative evaluation of filter aided sample preparation (FASP) and multienzyme digestion FASP protocols. *Anal. Chem* 88 (2016): 5438–5443.



This article is an open access article distributed under the terms and conditions of the [Creative Commons Attribution \(CC-BY\) license 4.0](https://creativecommons.org/licenses/by/4.0/)